CAPITAL UNIVERSITY OF SCIENCE AND TECHNOLOGY, ISLAMABAD

Reflection and Transmission Through Expansion Chamber Enclosed by Vertical Membranes

by

Rashid Ali

A thesis submitted in partial fulfillment for the degree of Master of Philosophy

in the

Faculty of Computing
Department of Mathematics

2019

Dedicated to my beloved father **Muhammad Anayat**.

CERTIFICATE OF APPROVAL

Reflection and Transmission Through Expansion Chamber Enclosed by Vertical Membranes

by

Rashid Ali

(MMT163012)

THESIS EXAMINING COMMITTEE

S. No.	Examiner	Name	Organization
(a)	External Examiner	Dr. Abdul Wahab	FAST NUCES, Islamabad
(b)	Internal Examiner	Dr. Shafqat Hussain	CUST, Islamabad
(c)	Supervisor	Dr. Muhammad Afzal	CUST, Islamabad

Dr. Muhammad Afzal
Thesis Supervisor
June, 2019

Dr. Muhammad Sagheer
Head
Dept. of Mathematics
June, 2019

Dr. Muhammad Abdul Qadir
Dean
Faculty of Computing
June, 2019

Author's Declaration

I Rashid Ali hereby state that my Master of Philosophy thesis titled "*Reflection and Transmission Through Expansion Chamber Enclosed by Vertical Membranes*" my own work and has not been submitted previously by me for taking any degree from Capital University of Science and Technology, Islamabad or anywhere else in the country/abroad.

At any time if my statement is found to be incorrect even after my graduation, the university has the right to withdraw my Master of Philosophy degree.

(Rashid Ali)

Registration No: MMT163012

Plagiarism Undertaking

I solemnly declare that research work presented in this thesis titled "*Reflection and Transmission Through Expansion Chamber Enclosed by Vertical Membranes*" is solely my research work with no significant contribution from any other person. Small contribution/help wherever taken has been dully acknowledged and that complete thesis has been written by me.

I understand the zero tolerance policy of the HEC and Capital University of Science and Technology towards plagiarism. Therefore, I as an author of the above titled thesis declare that no portion of my thesis has been plagiarized and any material used as reference is properly referred/cited.

I undertake that if I am found guilty of any formal plagiarism in the above titled thesis even after award of Master of Philosophy Degree, the University reserves the right to withdraw/revoke my Master of Philosophy Degree and that HEC and the University have the right to publish my name on the HEC/University website on which names of students are placed who submitted plagiarized work.

(Rashid Ali)

Registration No: MMT163012

Acknowledgements

All praise is for Allah, the Lord of the Worlds, who keeps us on the right path. I also yield witness that Prophet Muhammad(PBUH) is the last messenger of Allah whose life is a perfect model for whole mankind till the day of judgment. Allah helped me to continue my study and job togather. I could not do anything without the help of Allah.

First of all, I would like to thank my honorable adviser Assistant professor **Dr. Muhammad Afzal** for his continuous sincere support for my MPhil study and related research. His patience, motivation and immense knowledge gave me right path in research. He supported me all the time while completing the difficult thesis.

Besides of my adviser, I would also like to thank the rest faculty of department for their encouragement and insightful comments to widen my knowledge. They also enabled me to research in different fields of study. I could never fulfill my research without their precious support.

I would not forget my fellows who had worked hard togather and spent precious time in valuable discussion with me before deadlines. I would like to thank senior students who helped me in difficult times.

Last but not the least, I would thank to my father, wife, brothers, sisters and roommate friend for their spiritually support while writing the thesis.

(Rashid Ali)

Registration No: MMT163012

Abstract

In this dissertation, the reflection and transmission of acoustic waves through an expansion chamber enclosed by vertical membranes is presented. The mode-matching (MM) technique has been used to obtain the solution of boundary value problem. The solution is sorted by writing eigen expansions form of duct regions with unknown mode amplitudes. These unknowns are determined through matching conditions. The scattering powers are plotted against frequency for different values of membrane tension. It is found that variation of tension differs the scattering powers.

Contents

List of Figures

Chapter 1

Introduction

From last few decades, the noise pollution has become alarming to health of humans and environment. The main reason is the drastic increase of vehicles, huge building and industries. The noise pollution may disturb our minds, upset regular work or help in causing nervous and mental disorder. The indoor unwanted noise usually comes from the heating, ventilation and air conditioning (HVAC) units of buildings or aircraft. To reduce the environmental noise, by using different absorbent materials and geometrical designs of ducts is ongoing topic of modern research.

Acoustics is a field of science which deals with the generation, reception, transmission and reflection of pressure fluctuations. These fluctuations transport energy from one point of the medium to another point. The acoustic field has given many challenging and interesting problems to scientists and engineers. The continued interest is often motivated by necessity to design objects or channels that help to reduce the noise and related vibrations. The present thesis is related to the mathematical modelling of acoustic scattering in ducts or channels involving elastic membrane barriers. These boundary value problems are solved by using mode-matching technique. The detailed discussion of the thesis is presented in following chapters.

Chapter one includes the essential topics for thesis like important definitions, theories and governing laws. The material presented in this chapter is also available

in literature but here its inclusion will provide us suitable foundation for the work of the following chapters. This chapter also provides us information about the background data and the history of the problems discussed in this thesis.
In second Chapter, two problems of different geometries containing vertical membranes are discussed. First problem includes a continuous waveguide containing vertical membrane barrier at interface. However, the later problem involves additional step-discontinuity. The mathematical modeling and the solution methodologies of both problems are discussed in this chapter.
In third Chapter, the acoustic scattering through a two-dimensional rigid chamber enclosed by vertical membranes along with vertical step-discontinuity is presented. To find solution, the problem is divided into two sub-problems which are then solved one by one by using mode-matching technique.
In final Chapter 4, some concluding remarks are presented.

1.1 Acoustics

"Acoustics [16, 21] is the science of sound. It deals with the production of sound, the propagation of sound from the source to the receiver, and the detection and perception of sound. The word sound is often used to describe the two different things: an auditory sensation in the ear, and disturbance in a medium that can cause this sensation.
Acoustics has become a board interdisciplinary field encompassing the academic disciplines of physics, engineering, psychology, speech, audiology, music, architecture, physiology, neuroscience and others. Among the branches of acoustics are architectural acoustics, physical acoustics, musical acoustics, psycho acoustics, electroacoustics, noise control, shock and vibration, underwater acoustics, speech, physiological acoustics etc.
Sound can be produced by a number of different processes, which include the following.
Vibrating Bodies: when a drumhead or a noisy machine vibrates, it displaces air and causes the local air pressure to fluctuate.

Changing Air Flow: when we speak or sing, our vocal folds open or close to let through puffs of air. In a siren, holes on a rapidly rotating plate alternately pass and block air, resulting in a loud sound.
Time Dependent Heat Sources: on electrical spark produces a crackle, an explosion produces a bang due to expansion of air caused by rapid heating. Thunder results from rapid heating by a bolt of lightning.
Supersonic Flow: shock waves result when a supersonic airplane or a speeding bullet forces air to flow faster than the speed of sound."

1.2 Acoustic Wave Equation

The mathematical and physical aspects of disturbances or fluctuations can be discussed in term of second order partial differential equation which is called acoustic wave equation. To derive this acoustic wave equation, we assume the concept of continuum mechanics which consists of thermodynamic principle, conservation of mass and conservation of momentum. This equation can be found in the literature, for instant in, [16, 21].

1.2.1 Conservation of Mass

The differential form of the law of conservation of mass can be written as

$$\frac{\partial \rho}{\partial t} + \nabla . (\rho \mathbf{u}) = 0, \tag{1.1}$$

where, ρ and $\mathbf{u}$ are known as instantaneous mass density and velocity vector, respectively, of compressible fluid particles and $(\rho \mathbf{u}).\mathbf{n}$ is the net mass flowing per unit time per unit area across any arbitrary stationary surface within material whose local unit onward normal vector is $\mathbf{n}$. It is also known as the continuity equation.

1.2.2 Conservation of Momentum

The momentum equation for incompressible flow of a Newtonian fluid can be written as

$$\frac{\partial (\rho \mathbf{u})}{\partial t} = -\nabla . (\rho \mathbf{u}) \mathbf{u} - \nabla p + \rho \bar{g}, \tag{1.2}$$

where p, $\bar{g}$, ∇p, $\rho \bar{g}$ and μ denote the pressure, gravitational acceleration, exerting pressure, body forces and viscosity, respectively. From (1.2), we can write

$$\rho \frac{D\mathbf{u}}{Dt} = -\nabla p + \rho \bar{g}, \tag{1.3}$$

which is also called as Euler's equation, where

$$\frac{D}{Dt} = \frac{\partial}{\partial t} + \mathbf{u}.\nabla,$$

is known as Stoke's total time derivative [1] in which first and second terms show time derivative and convective term, respectively.

1.2.3 Thermodynamic Principle

The equation of state for Ideal gas can be written as

$$p = \rho r T, \tag{1.4}$$

where p, ρ, r and T represent pressure, density, gas constant and temperature, respectively. The equation for perfect gas enclosed by conductive vessel is given as

$$\frac{p}{p_0} = \frac{\rho}{\rho_0}. \tag{1.5}$$

If there is no heat entered or lost by the vessel then

$$\frac{p}{p_0} = \left(\frac{\rho}{\rho_0}\right)^{\gamma}, \tag{1.6}$$

where, $\gamma = C_p/C_v$ shows ratio in heat capacities of constant pressure and constant volume. The condensation s of gas is defined as

$$s = \frac{\rho - \rho_0}{\rho_0}. \tag{1.7}$$

From (1.6) and (1.7), we may get

$$\frac{p}{p_0} = (1 + s)^{\gamma}. \tag{1.8}$$

On expanding (1.8) by Binomial series, we get

$$p - p_0 = p_0 \gamma s + O(s^2). \tag{1.9}$$

According to Taylor's series, p is expanded over ρ_0, that is

$$p = p_0 + \left(\frac{\partial p}{\partial \rho}\right)_{\rho=\rho_0} (\rho - \rho_0) + O(s^2). \tag{1.10}$$

On using (1.7) into (1.10), we get

$$p - p_0 = \rho_0 \left(\frac{\partial p}{\partial \rho}\right)_{\rho=\rho_0} s + O(s^2). \tag{1.11}$$

Due to small fluctuation in vessel, second and higher order terms of s are neglected. Therefore, after comparing (1.9) and (1.11), we get

$$\gamma p_0 = \rho_0 \left(\partial p/\partial \rho\right)_{\rho=\rho_0}. \tag{1.12}$$

Therefore, (1.11) can also be written as

$$P = \beta s, \tag{1.13}$$

which is equation of acoustic pressure where, $\beta = \rho_0 \left(\partial p/\partial \rho\right)_{\rho=\rho_0}$ and $P = p - p_0$ are the adiabatic bulk modulus and pressure perturbation, respectively.

1.2.4 Linearization

To linearize the equations for perfect ideal fluid, we put $\rho = \rho_0 + \rho_0 s$ into (1.1) to get

$$\frac{\partial s}{\partial t} + \nabla.\mathbf{u} = 0. \tag{1.14}$$

Likewise, on substituting $\rho = \rho_0 + \rho_0 s$ and $P = p - p_0$ into (1.3), after neglecting body forces, (1.3) can be linearized as

$$\rho_0 \frac{\partial \mathbf{u}}{\partial t} = -\nabla P, \tag{1.15}$$

where, ρ_0, P and P_0 are the ambient density, pressure perturbation and ambient pressure, respectively. By taking divergence of (1.15), we get

$$\rho_0 \frac{\partial \nabla.\mathbf{u}}{\partial t} = -\nabla^2 P. \tag{1.16}$$

On differentiating (1.14) with respect to t, we obtain

$$\frac{\partial^2 s}{\partial t^2} = -\frac{\partial(\nabla.\mathbf{u})}{\partial t}. \tag{1.17}$$

By comparing (1.16) and (1.17), we found

$$\rho_0 \frac{\partial^2 s}{\partial t^2} = \nabla^2 P. \tag{1.18}$$

On invoking (1.13) into (1.18), we get

$$\frac{\partial^2 P}{\partial t^2} = \frac{1}{c^2}\nabla^2 P, \tag{1.19}$$

which is the linearized acoustic wave equation in pressure form with speed of sound or phase speed c, where $c^2 = \beta/\rho_0$. The phase speed or speed of sound c can be obtained by using the properties of medium e.g. for air we use $c = 344ms^{-1}$.

1.3 Membrane

A lamina or plate containing negligible bending resisting when it is subjected to tension is known as membrane; e.g., drumhead. The equation of vibrating membrane can be found in many texts, see for example [16, 21]. Here, a short detail on derivation is given.

1.3.1 Equation of Motion of Vibrating Membrane

A homogeneous and perfectly flexible membrane bounded by a curve in xy-plane is as shown in Figure 1.1.

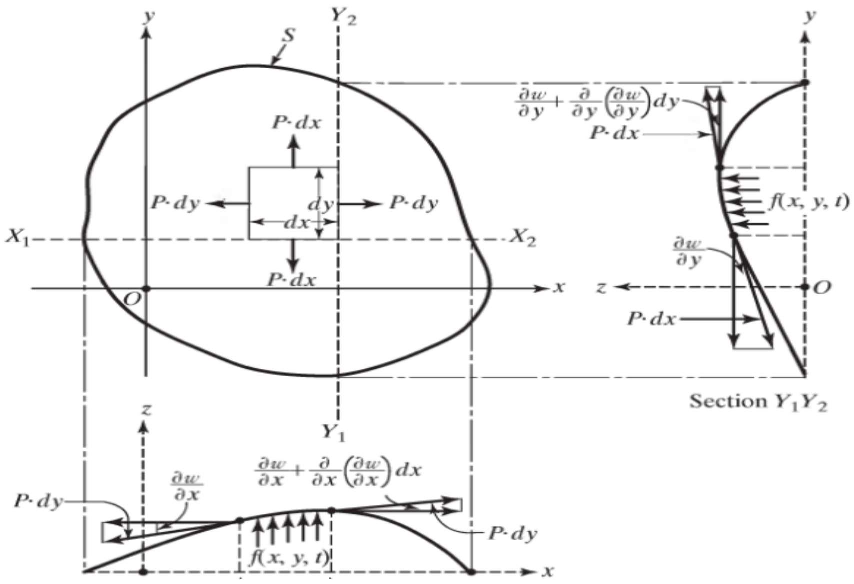

Figure 1.1: Vibrating membrane.

To derive equation of motion of a membrane, we let displacement w and deflection $\partial w/\partial x$ in x-direction. After applying force, the displacement becomes $w + \frac{\partial w}{\partial x}dx$ and deflection becomes $\frac{\partial}{\partial x}\left(w + \frac{\partial w}{\partial x}dx\right)$ in x-direction.

Likewise in y-direction, we let displacement w and deflection $\partial w/\partial y$, which after applying force in y-direction, become $w + \partial w/\partial y dy$ and $\partial/\partial y\,(w + \partial w/\partial y dy)$, respectively. The force acting along x-direction can be given as

$$-Pdy\frac{\partial w}{\partial x} + Pdy\frac{\partial}{\partial x}\left(w + \frac{\partial w}{\partial x}dx\right) = P\frac{\partial^2 w}{\partial x^2}dxdy. \tag{1.20}$$

Similarly along y-direction, the net force is

$$-Pdx\frac{\partial w}{\partial y}+Pdx\frac{\partial}{\partial y}\left(w+\frac{\partial w}{\partial y}dy\right)=P\frac{\partial^2 w}{\partial y^2}dxdy. \tag{1.21}$$

If $\rho(x,t)$ is the mass per unit area of the path then mass $M=\rho dxdy$ and thus inertial force will take the form

$$\rho dxdy\frac{\partial^2 w}{\partial t^2}. \tag{1.22}$$

According to Newton second's law

$$Pdxdy\frac{\partial^2 w}{\partial x^2}+Pdxdy\frac{\partial^2 w}{\partial y^2}=\rho dxdy\frac{\partial^2 w}{\partial t^2}, \tag{1.23}$$

which after simplification yields

$$\left(\frac{\partial^2 w}{\partial x^2}+\frac{\partial^2 w}{\partial y^2}\right)=\frac{1}{c^2}\frac{\partial^2 w}{\partial t^2}, \tag{1.24}$$

where $c=(P/\rho)^{1/2}$. The equation of motion with forcing $f(x,y,t)$ can be given as

$$\left(\frac{\partial^2 w}{\partial x^2}+\frac{\partial^2 w}{\partial y^2}\right)+f(x,y,t)=\frac{1}{c^2}\frac{\partial^2 w}{\partial t^2}, \tag{1.25}$$

which is also called two dimensional wave equation.

1.4 Waveguide

"A waveguide is a structure that guides waves, such as electromagnetic waves or sound, with minimal loss of energy by restricting expansion to one-dimensional or two. The geometry of a waveguide represents its function. For example, water waves constrained with in a canal, or guns that have barrels which restricted hot gas expansion to maximize energy transfer to their bullets etc are waveguides. An acoustic waveguide behaves like a transmission line in which sound waves propagate."

1.5 History and Literature Review

In the 6th century BC, Pythagoras [11] worked over musical sounds and vibrating strings. Pythagoras found that consonant musical intervals were produced through vibrating strings. He studied about pitch of string produced due to tension. The Roman architect Vitruvius worked over the designs of acoustical theaters. Vitruvius selected a site in which sound transmission lost smoothly and did not come back after reflection so it did not become harmful to ears. Galileo discussed about the relationship of pitch of a vibrating string to its length. Sauveur made complete study about the relationship of frequency to pitch. The English mathematician Taylor presented the solution for the frequency of the vibrating string in its fundamental mode. Bernoulli provided partial differential equation for the vibrating string and obtained its solution through d'Alembert principle. Poisson discussed first time the solution of vibrational membrane. Clench discussed about the solution for vibrating circular membrane. Chaldeni informed about the solution of vibrating plate in 1787.
In the 19th century, Tyndall worked over transmission of sound in atmosphere and combinations of musical tones. Tyndall observed that longitudinal vibration was produced by rubbing a rod. Tyndall obtained a waveform of musical sound. He noted the effects of fog and water in various weather conditions on the transmission of sound. Helmholtz improved the work of Tyndall by working over the quality of musical sound. He separated the components of unfair tones. Helmholtz derived that quality of sound depended upon the strength of partial tone. Helmholtz invented a vibrational microscope. Stokes presented a three-dimensional equation of motion of a viscous fluid which was known as Stokes-Naiver equation. So the propagation of sound waves could be found by this Stokes-Naiver equation. In 1876, Bell invented a microphone which was later known as a telephone. In 1877, Edison invented the first phonograph. Edison recorded first time human voice for posterity. Koening created all kinds of tuning forks. Scheibler formed a set of forks called tonometer which controlled the frequency in small steps. Koening formed a tonometer of 154 forks which controlled frequency ranging from 16Hz

to 21845Hz. Koening made cylindrical and spherical Helmholtz [2] resonators of different kinds.

In 20th century, Sabine [3], father of architectural acoustics, measured quantity of sound in the room and made acoustical theaters. Rayleigh and Strutt [4] found a way to measure the intensity of a sound source. Knudsen and Harris [9] improved the work of Sabine by invetigating the effects of molecular relaxation phenomena in gases and liquid. In 1940, Bolt with the help of Bernanke and Martin [12] worked over the acoustical building, halls, Musical Sheds and centers for performing art. Langevin used echo ranging to detect mines in World War-1. Mckinney [19] used Sonar for military applications. Lighthill [7] studied about non-linear acoustics in fluid. Hamilton and Blackstock [13], and Beyer [6] investigated the propagation of sound through liquids, gases or solids. Rott [8] analyzed the sound propagation in gases with an axial temperature gradient. Cumming and Chung [10] imposed matching condition at interfaces of waveguides.

From last few decades Haung [18], Haung and Choy [20] used different aspects of channels for distortion of fan noise in HVAC system. They worked over different geometrical channels containing membranes. Lawrie and Abrahams [14] investigated about boundary value problems and used orthogonality relation to solve the difficult integrals. Warren *et al.* [17] analyzed about scattering in different geometrical channels with different material properties. Haung [15] analyzed drum like silencer and reflection of sound waves through chamber enclosed by vertical plates. Nawaz and Lawrie [23] discussed about the scattering through elastic plate bounded ducts at flanged junctions. Kim *et al.* [24] gave solution of scattering through double vertical plates present in a continuous duct. Lawrie and Afzal studied different geometrical channels bounded above by membranes. Noble [5] used a Wiener- Hopf technique to solve different geometrical channels with different material. This technique was much succeeded but failed to solve most complicated channels. Lawrie [22] solved most complicated channels having membranes 3 mode-matching method.

Now in recent years, the mode-matching technique is being used to solve most complicated waveguides. In this thesis, I have gotten the motivation from the work done by Kim *et al.* [24] and presented analysis with double vertical membranes instead of vertical plates. The idea of mode-matching approach presented in the thesis has been taken from Afzal and Lawrie [25].

Chapter 2

Reflection and Transmission Through a Vertical Membrane Barrier

In this chapter, we include two problems containing different geometrical configurations. In first problem, the propagation and scattering of acoustic waves through an infinite waveguide having finite vertical membrane barrier at interface, is discussed. However, the later problem involves additional step-discontinuity at the interface. The upper and lower walls of the problems are assumed to be rigid. The mode-matching technique is applied to solve the modeled problems and then energy conservation is discussed. At the end, numerical results are debated.

2.1 Scattering Through a Vertical Membrane in Continuous Waveguide

Here, we consider a two-dimensional infinite waveguide in dimensional rectangular plane $(\bar{x}, \bar{y})$, containing finite vertical membrane barrier at interface. It is pertinent to mention here that the over bars with variables henceforth stand for the dimensional setting of coordinates. A vertical membrane of height $\bar{a}$ lying along

$\bar{x} = 0$ divide the waveguide into two semi-infinite duct regions. The inside of the waveguide is filled with compressible fluid of density ρ and sound speed c while outer side of it is in *vacuo*. The physical configuration of the waveguide is as shown in Figure 2.1.

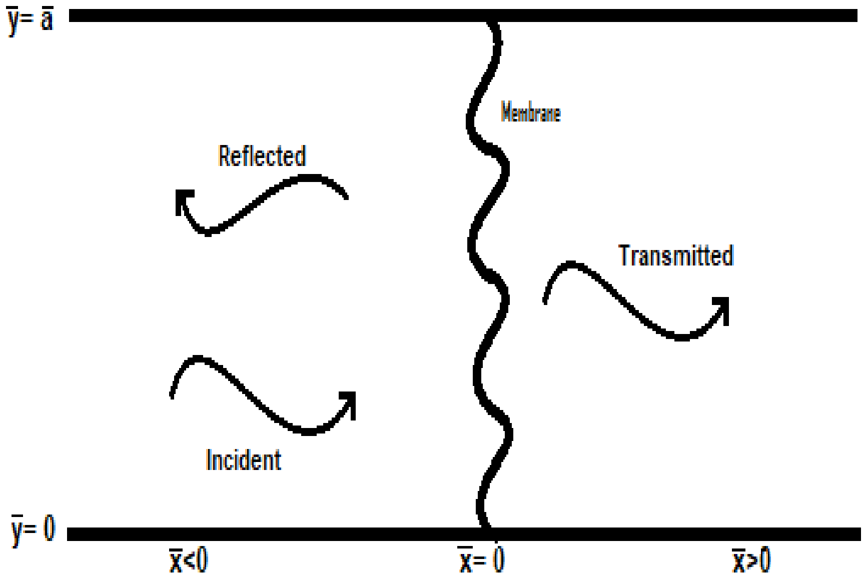

Figure 2.1: The physical geometry of problem-1.

Consider an incident wave from negative x-direction is propagating towards the membrane barrier which after imping with the barrier will scatter into infinite number of reflected and transmitted modes. The propagation and scattering of acoustic waves in the waveguide can be discussed by using the wave equation that is,

$$\frac{\partial^2 \bar{\Phi}}{\partial \bar{x}^2} + \frac{\partial^2 \bar{\Phi}}{\partial \bar{y}^2} = \frac{1}{c^2} \frac{\partial^2 \bar{\Phi}}{\partial \bar{t}^2}, \tag{2.1}$$

where $\bar{\Phi}(\bar{x}, \bar{y}, \bar{t})$ denotes the dimensional velocity potential in the waveguide. The acoustically rigid boundaries of the waveguide are defined by

$$\frac{\partial \bar{\Phi}}{\partial \bar{y}} = 0, \quad \bar{y} = 0, \bar{a}. \tag{2.2}$$

As there is an elastic membrane lying at interface $\bar{x} = \bar{0}$ which can be given mathematically as

$$\frac{\partial^2 \bar{W}}{\partial \bar{y}^2} - \frac{1}{c_m^2} \frac{\partial^2 \bar{W}}{\partial \bar{t}^2} = \frac{1}{\mathrm{T}} [\bar{P}]_-^+, \tag{2.3}$$

where, $[\bar{P}]_{-}^{+} = \bar{P}^{+} - \bar{P}^{-}$ denotes the acoustic pressure across the regions in which $\bar{P}$ is pressure purturbation. The quantity $c_m = (\mathrm{T}/\rho_m)^{\frac{1}{2}}$ represents the speed of waves on membrane containing density ρ_m and tension T. Note that the pressure purturbation $\bar{P}$ and membrane displacement $\bar{W}(\bar{y}, \bar{t})$ are related to the velocity potential $\bar{\Phi}(\bar{x}, \bar{y}, \bar{t})$ by the relation

$$\bar{P} = -\rho \frac{\partial \bar{\Phi}}{\partial \bar{t}}, \tag{2.4}$$

$$\frac{\partial \bar{W}}{\partial \bar{t}} = \frac{\partial \bar{\Phi}}{\partial \bar{x}}. \tag{2.5}$$

On assuming the harmonic time dependence $e^{-i\omega\bar{t}}$, it is convenient to express the velocity potential and membrane displacement by

$$\bar{\Phi}(\bar{x}, \bar{y}, \bar{t}) = \bar{\psi}(\bar{x}, \bar{y}) e^{-i\omega\bar{t}}, \tag{2.6}$$

and

$$\bar{W}(\bar{y}, \bar{t}) = \bar{w}(\bar{y}) e^{-i\omega\bar{t}}, \tag{2.7}$$

respectively. Here, $\bar{\psi}(\bar{x}, \bar{y})$ and $\bar{w}(\bar{y})$ are the dimensional time independent velocity potential and membrane displacement, respectively. On using (2.6) into (2.1), we get the Helmholtz equation

$$\left(\frac{\partial^2}{\partial \bar{x}^2} + \frac{\partial^2}{\partial \bar{y}^2} + k^2 \right) \bar{\psi}(\bar{x}, \bar{y}) = 0, \tag{2.8}$$

where $k = \omega/c$ is the wave number. Now first we put (2.4) into (2.3) to get

$$\frac{\partial^2 \bar{W}}{\partial \bar{y}^2} - \frac{1}{c_m^2} \frac{\partial^2 \bar{W}}{\partial \bar{t}^2} = \frac{-\rho}{T} \left[\frac{\partial \bar{\Phi}}{\partial \bar{t}} \right]_{-}^{+}, \tag{2.9}$$

then on using (2.6) and (2.7), we find

$$\frac{\partial^2 \bar{w}}{\partial \bar{y}^2} + \frac{\omega^2}{c_m^2} \bar{w} = \frac{i\omega\rho}{T} [\bar{\psi}]_{-}^{+}. \tag{2.10}$$

However, since

$$\bar{w} = \frac{i}{\omega} \frac{\partial \bar{\psi}}{\partial \bar{x}}, \tag{2.11}$$

(2.10) becomes

$$\left[\frac{\partial^2}{\partial \bar{y}^2} + \frac{\omega^2}{c_m^2}\right]\frac{\partial \bar{\psi}}{\partial \bar{x}} = \frac{\omega^2 \rho}{T}\left[\bar{\psi}\right]_-^+. \tag{2.12}$$

We non-dimensionalize the above equations with respect to the length scale k^{-1} and time scale ω^{-1} under the transformations given by $\bar{\psi} = \frac{\omega}{k^2}\psi$, $k\bar{x} = x$, $k\bar{y} = y$ and $\omega\bar{t} = t$. The non-dimensional form of above equation (2.2), (2.8) and (2.12) is found to be

$$\left(\frac{\partial^2}{\partial x^2} + \frac{\partial^2}{\partial y^2} + 1\right)\psi\left(x, y\right) = 0, \tag{2.13}$$

$$\frac{\partial \psi}{\partial y} = 0, \quad y = 0, a, \tag{2.14}$$

$$\left\{\frac{\partial^2}{\partial y^2} + \mu^2\right\}\frac{\partial \psi}{\partial x} - \alpha\left[\psi\right]_-^+ = 0, \tag{2.15}$$

where, $\mu = c/c_m$ and $\alpha = c^2\rho/\left(k\mathrm{T}\right)$ are the wave number and fluid loading parameters, respectively. For convenience, we may write the velocity potential ψ as

$$\psi(x, y) = \begin{cases} \psi_1\left(x, y\right), & x < 0, \quad 0 \leqslant y \leqslant a \\ \psi_2\left(x, y\right), & x > 0, \quad 0 \leqslant y \leqslant a, \end{cases} \tag{2.16}$$

where, $\psi_1\left(x, y\right)$ and $\psi_2\left(x, y\right)$ represent the velocity potential in left hand region $(x < 0, 0 \leqslant y \leqslant a)$ and the right hand region $(x > 0, 0 \leqslant y \leqslant a)$, respectively.

Let us assume an incident wave present in the left hand duct and calculate the reflected and transmitted fields by using mode-matching technique. For this, we first determine the eigenfunction expression forms of field potentials via separation of variable approach. Thus, we assume

$$\psi(x, y) = X(x)Y(y). \tag{2.17}$$

On using (2.17) into (2.13), it is straightforward to obtain

$$\left(\frac{Y''}{Y} + 1\right) = -\frac{X''}{X} = -\eta^2, \tag{2.18}$$

which yields

$$Y'' + \tau^2 Y = 0, \tag{2.19}$$

and

$$X'' + \eta^2 X = 0, \tag{2.20}$$

where, $\tau = \sqrt{1-\eta^2}$. On solving (2.20) and (2.19), we get

$$Y_n(y) = c_1 \cos(\tau y) + c_2 \sin(\tau y), \tag{2.21}$$

and

$$X_n(x) = c_3 e^{i\eta x} + c_4 e^{-i\eta x}, \tag{2.22}$$

respectively. From the rigid boundary condition (2.14), we found that

$$Y'(y) = 0, \quad y = 0, a, \tag{2.23}$$

where prime denotes the differentiation with respect to y. On using (2.21) into (2.23), we get

$$\sin(\tau a) = 0, \tag{2.24}$$

for non-trivial solution, which yields the eigen values of the eigen system as $\tau = \tau_n = \frac{n\pi}{a}; n = 0, 1, 2, \ldots$. The corresponding eigenfunctions will take the form $y_n = \cos(\tau_n y); n = 0, 1, 2, \ldots$. These eigenfunctions determine the shape of propagating mode with rigid boundaries. Therefore, the n^{th} propagating mode of duct region can be expressed by

$$\psi_n(x, y) = \left(F_n e^{i\eta_n x} + A_n e^{-i\eta_n x}\right) \cos(\tau_n y), \tag{2.25}$$

where, the coefficient F_n and A_n are the amplitudes of n^{th} mode. Note that first term in (2.25) denotes the n^{th} mode propagating in positive x-direction while second term represents the n^{th} mode propagating toward negative x-direction. Now from superposition principle, the total field in the duct regions is

$$\psi = \sum_{n=0}^{\infty} \psi_n(x, y). \tag{2.26}$$

Therefore, we may write for left hand duct

$$\psi_1(x,y) = \sum_{n=0}^{\infty} F_n e^{i\eta_n x} \cos(\tau_n y) + \sum_{n=0}^{\infty} A_n e^{-i\eta_n x} \cos(\tau_n y), \tag{2.27}$$

and for right hand duct

$$\psi_2(x,y) = \sum_{n=0}^{\infty} B_n e^{i\eta_n x} \cos(\tau_n y). \tag{2.28}$$

Note that first term on the right hand side of (2.27) denotes the incident field with forcing F_n (that will be defined later) while the second term in (2.27) represents the reflected field. However, (2.28) gives transmitted field.
Also the quantities $\{A_n, B_n\}$; $n = 0, 1, 2, \ldots$ in (2.27) and (2.28) are the amplitudes and are unknowns. To determine these unknowns, we match the normal velocities and pressure modes across the region at interface $x = 0$. The process of Mod-Matching is discussed in the next section.

2.1.1 Mode-matching

From the continuity of normal velocities at interface, we may write

$$\frac{\partial \psi_1}{\partial x} = \frac{\partial \psi_2}{\partial x}, \quad x = 0, \quad 0 \leqslant y \leqslant a. \tag{2.29}$$

On using (2.27) and (2.28) into (2.29), we found

$$\sum_{n=0}^{\infty} B_n \eta_n \cos(\tau_n y) = \sum_{n=0}^{\infty} \{F_n - A_n\} \eta_n \cos(\tau_n y). \tag{2.30}$$

On multiplying (2.30) with $\cos(\tau_m y)$ and integrating over $0 \leqslant y \leqslant a$, we get

$$\begin{aligned}\sum_{n=0}^{\infty} B_n \eta_n \int_0^a \cos(\tau_n y)\cos(\tau_m y)dy &= \sum_{n=0}^{\infty} F_n \eta_n \int_0^a \cos(\tau_m y)\cos(\tau_n y)dy \\ &- \sum_{n=0}^{\infty} A_n \eta_n \int_0^a \cos(\tau_n y)\cos(\tau_m y)dy. \end{aligned}\tag{2.31}$$

As $\cos(\tau_m y); m = 0, 1, 2, ...$ are orthogonal in nature which satisfies the orthogonality relation

$$\int_0^a \cos(\tau_m y)\cos(\tau_n y)dy = \frac{a}{2}\delta_{mn}\varepsilon_m, \tag{2.32}$$

where δ_{mn} is Kronecker delta and $\varepsilon_m = 2$, for $m = 1$ and $\varepsilon_m = 1$, for $m \neq 0$. On using (2.32), (2.31) yields

$$A_m = F_m - B_m. \tag{2.33}$$

Now with the aid of (2.33), we may rewrite the eigen expression for left hand duct in term of transmitted amplitudes $B_m; m = 0, 1, 2...$, as

$$\psi_1 = \sum_{n=0}^{\infty} F_n \cos(\tau_n y)\left\{e^{-i\eta_n x} + e^{i\eta_n x}\right\} - \sum_{n=0}^{\infty} B_n e^{-i\eta_n x}\cos(\tau_n y). \tag{2.34}$$

To discuss the vertical membrane barrier at interface, we impose condition

$$\left(\frac{\partial^2}{\partial y^2} + \mu^2\right)\frac{\partial \psi_2}{\partial x} - \alpha\left(\psi_2 - \psi_1\right) = 2\delta(y)E_1 + 2\delta\left(y - a\right)E_2,$$
$$x = 0, 0 \leqslant y \leqslant a. \tag{2.35}$$

Here $\delta(.)$ is the Dirac delta function which is used here to impose two extra conditions on the vertical membrane's edges at $x = 0, y = 0, a$, where, E_1 and E_2 are constants. These constants define the connection of membrane with edges. Now on using (2.28) and (2.34) into (2.35), we get

$$\sum_{n=0}^{\infty} B_n\left[i\eta_n\left(\mu^2 - \tau_n^2\right) - 2\alpha\right]\cos(\tau_n y) + 2\alpha\sum_{n=0}^{\infty} F_n\cos(\tau_n y)$$
$$= 2\delta(y)E_1 + 2\delta\left(y - a\right)E_2. \tag{2.36}$$

On multiplying with $\cos(\tau_m y)$, integrating over $0 \leqslant y \leqslant a$ and then using orthogonality relation (2.32), we get after simplification

$$B_m = \frac{-2\alpha F_m}{\Delta_m} + \frac{2E_1}{a\varepsilon_m\Delta_m} + \frac{2E_2(-1)^m}{a\varepsilon_m\Delta_m}, \tag{2.37}$$

where

$$\Delta_m = i\eta_m\left(\mu^2 - \tau_m^2\right) - 2\alpha.$$

Note that the constants E_1 and E_2 are still unknowns. These are determined through the physical connection of vertical membrane with horizontal rigid plates. Let us assume here the edges to be fixed, thus displacement is zero, that is

$$\frac{\partial \psi_2}{\partial x} = 0, \quad x = 0, \quad y = 0 \tag{2.38}$$

and

$$\frac{\partial \psi_2}{\partial x} = 0, \quad x = 0, \quad y = a. \tag{2.39}$$

On differentiating (2.28) with respect to x, we found

$$\psi_{2x}(x, y) = i \sum_{m=0}^{\infty} B_m e^{i\eta_m x} \eta_m \cos(\tau_m y). \tag{2.40}$$

On using (2.40) into (2.38) and (2.39), we obtain

$$\sum_{m=0}^{\infty} iB_m \eta_m = 0, \tag{2.41}$$

and

$$\sum_{m=0}^{\infty} iB_m \eta_m (-1)^m = 0. \tag{2.42}$$

To enforce (2.41), we multiply (2.37) with $\sum_{m=0}^{\infty} i\eta_m$ and then use (2.41), which after simplification yields

$$S_1 E_1 + S_2 E_2 = \sum_{m=0}^{\infty} \eta_m \left\{ 2i\alpha F_m - B_m \eta_m \left(\mu^2 - \tau_m^2\right) \right\}, \tag{2.43}$$

where

$$S_1 = \sum_{m=0}^{\infty} \frac{2i\eta_m}{a\varepsilon_m},$$

and

$$S_2 = \sum_{m=0}^{\infty} \frac{2i\eta_m}{a\varepsilon_m} (-1)^m.$$

To enforce (2.42), we multiply (2.37) with $\sum_{m=0}^{\infty} i\eta_m(-1)^m$ and then use (2.42) to get

$$S_2E_1 + S_1E_2 = \sum_{m=0}^{\infty} \eta_m(-1)^m \left\{2i\alpha F_m - B_m\eta_m\left(\mu^2 - \tau_m^2\right)\right\}. \tag{2.44}$$

In this way, E_1 and E_2 are found after solving (2.43) and (2.44) simultaneously. Now, if we assume the incident forcing $F_m = \delta_{m0}$, which cater only the fundamental duct mode to be incident, the expressions (2.33) and (2.37) will yield the reflected and transmitted amplitudes, respectively.

2.1.2 Energy Conservation

The reflected and transmitted fields can be discussed in terms of energy flux/power. The expression for power/energy flux is defined by (see, for example, [17])

$$P = \frac{1}{2}Re\left[i\int_R \psi\left(\frac{\partial\psi}{\partial\mathbf{n}}\right)^* dR\right], \tag{2.45}$$

where $(*)$ indicates the complex conjugate and $\mathbf{n}$ represents the normal to the region. Here, the incident field with forcing $F_n = \delta_{no}$ is $\psi_{inc}(x,y) = e^{ix}$, which on using into (2.45) leads to the incident power

$$P_i = \frac{1}{2}Re\left[i\int_0^a e^{ix}\left(-ie^{-ix}\right)dy\right], \tag{2.46}$$

which after simplification yields

$$P_i = \frac{a}{2}. \tag{2.47}$$

Likewise, for reflected field

$$\psi_r(x,y) = \sum_{n=0}^{\infty} A_n\cos(\tau_n y)e^{-i\eta_n x}, \tag{2.48}$$

we substitute (2.48) into (2.45) to get

$$P_r = -\frac{1}{2}Re\left\{\int_0^a \sum_{n=0}^{\infty}\sum_{m=0}^{\infty} A_n\eta_n^*\cos(\tau_n y)A_n^*\cos(\tau_m y)e^{-i(\eta_n-\eta_n^*)}dy\right\}. \tag{2.49}$$

On using orthogonality relation (2.32) into (2.49), we get

$$P_r = -\frac{a}{4} Re \left[\sum_{n=0}^{\infty} \mid A_n \mid^2 \varepsilon_n \eta_n \right]. \tag{2.50}$$

Likewise, the transmitted field is

$$\psi_t(x, y) = \sum_{n=0}^{\infty} B_n \cos(\tau_n y) e^{i\eta_n x}. \tag{2.51}$$

On using (2.51) into (2.45), which after simplification leads to

$$P_t = -\frac{1}{2} Re \int_0^a \sum_{n=0}^{\infty} \sum_{m=0}^{\infty} B_n \, (\eta_n^*) \cos(\tau_n y) B_n^* \cos(\tau_m y) dy. \tag{2.52}$$

On using orthogonality relation (2.32), we found

$$P_t = \frac{a}{4} Re \left[\sum_{n=0}^{\infty} \mid B_n \mid^2 \varepsilon_n \eta_n \right]. \tag{2.53}$$

For any enclosure, the left hand power is equal to the right hand that is

$$P_i + P_r = P_t. \tag{2.54}$$

On using (2.47), (2.50) and (2.53), (2.54) yields

$$\frac{a}{2} - \frac{a}{4} Re \left[\sum_{n=0}^{\infty} \mid A_n \mid^2 \varepsilon_n \eta_n \right] = \frac{a}{4} Re \left[\sum_{n=0}^{\infty} \mid B_n \mid^2 \varepsilon_n \eta_n \right]. \tag{2.55}$$

Now by dividing $2/a$ on both sides of (2.55), we obtain

$$1 = \frac{1}{2} Re \left[\sum_{n=0}^{\infty} \mid B_n \mid^2 \varepsilon_n \eta_n \right] + \frac{1}{2} Re \left[\sum_{n=0}^{\infty} \mid A_n \mid^2 \varepsilon_n \eta_n \right]. \tag{2.56}$$

We may scale (2.56) the incident power to unity, that is,

$$1 = \mathcal{E}_r + \mathcal{E}_t, \tag{2.57}$$

which is the conserved power identity, where

$$\mathcal{E}_r = \frac{1}{2} Re \left[\sum_{n=0}^{\infty} \mid A_n \mid^2 \varepsilon_n \eta_n \right] \tag{2.58}$$

and

$$\mathcal{E}_t = \frac{1}{2} Re \left[\sum_{n=0}^{\infty} \mid B_n \mid^2 \varepsilon_n \eta_n \right]. \tag{2.59}$$

Note that (2.58) and (2.59) denote reflected and transmitted power components for which the incident power is being scaled at unity.

2.1.3 Numerical Results

Here, the problem considered in previous section is discussed numerically.

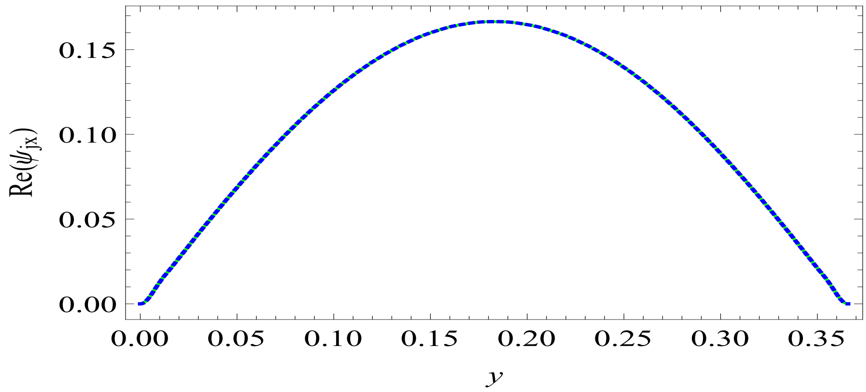

Figure 2.2: Real part of normal velocity plotted against duct height y, where $\bar{a} = 0.08$.

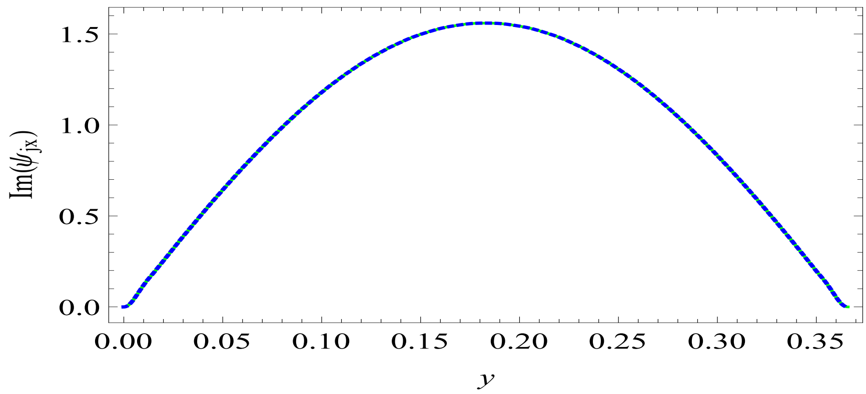

Figure 2.3: Imaginary part of normal velocity plotted against duct height y, where $\bar{a} = 0.08$.

Therefore, first we truncate the infinite system of equations defined by (2.33) and (2.37) along with (2.43) and (2.44) upto $n = m = 0, 1, 2, \ldots, N$ terms. It clearly reveals $N + 1$ equations. To draw the results graphically, consider the system is truncated upto $N = 50$ terms. The density of compressible fluid $\rho = 1.2Kg\ m^{-3}$ and speed of sound $c = 344m\ s^{-1}$ are assumed. The membrane mass density $\rho = 0.1715Kg\ m^{-2}$ and dimensional duct height $\bar{a} = 0.08$ remain fixed. Now for fixed frequency $f = 250$Hz, the real and imaginary parts of normal velocities against non-dimensional duct height at interface are illustrated in the Figures 2.2 and 2.3, respectively. It can be seen that both the curves coincide which clearly reveals that the truncated solution reconstructs exactly the matching condition (2.29). Moreover, it confirms the accuracy of the performed algebra.

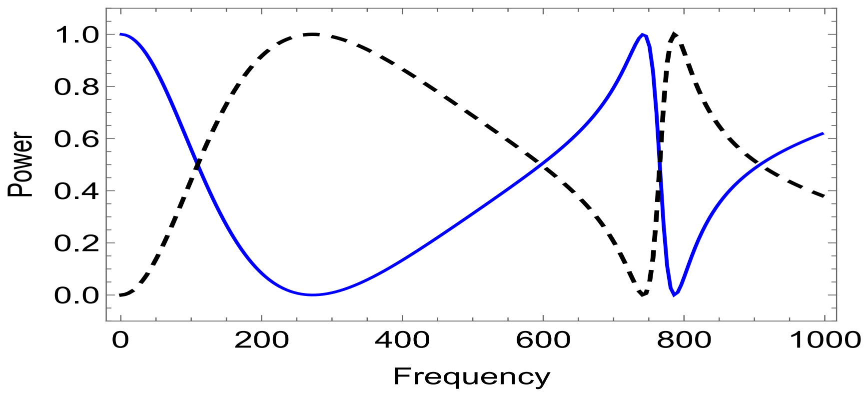

Figure 2.4: Reflected power $\mathcal{E}_r$ (solid line) and transmitted power $\mathcal{E}_t$ (dashed line) against frequency for tension $\mathrm{T} = 350\mathtt{N}$, where $\bar{a} = 0.085$

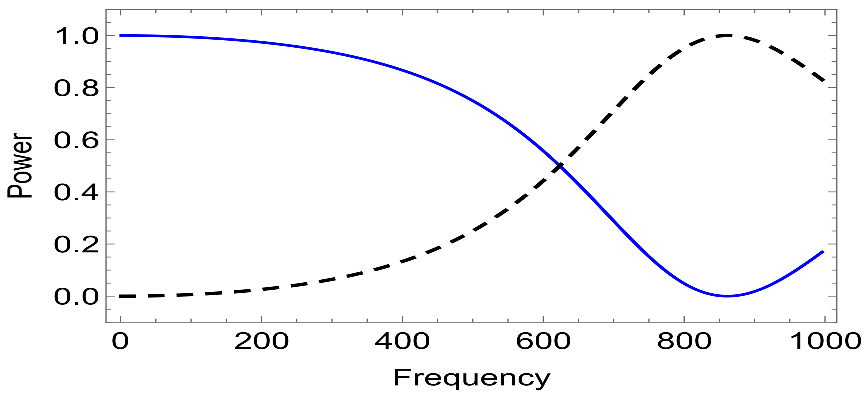

Figure 2.5: Reflected power $\mathcal{E}_r$ (solid line) and transmitted power $\mathcal{E}_t$ (dashed line) against frequency for tension $\mathrm{T} = 3500\mathtt{N}$, where $\bar{a} = 0.085$.

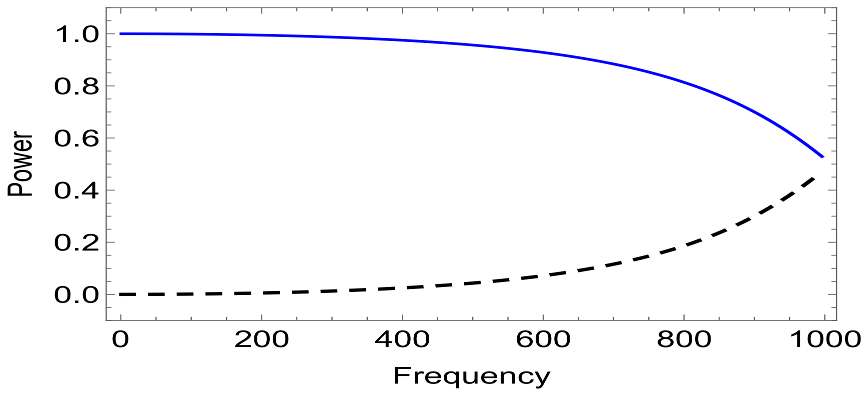

Figure 2.6: Reflected power $\mathcal{E}_r$ (solid line) and transmitted power $\mathcal{E}_t$ (dashed line) against frequency for tension $\mathrm{T} = 7500\mathtt{N}$, where $\bar{a} = 0.085$.

To understand the problem physically, the reflected and transmitted powers are plotted against frequency for different values of tension. It can be seen that, by varying frequency from 1Hz to 1000Hz, a significant variation in power components is noted. Also, by changing the tension T of the membrane, the dip points are varied. Moreover the sum of reflected and transmitted powers is unity as assumed in (2.57). It clearly justifies the conservation of power computationally as shown in the Figures 2.4, 2.5 and 2.6.

2.2 Scattering Through a Vertical Membrane in Discontinuous Waveguide

Here, we extend the geometrical configuration discussed in previous section with an inclusion of an additional rigid step-discontinuity at interface. It changes the height of second duct region from the first region. Note that the boundary value problem for this case is same as defined in previous section. The inclusion of step-discontinuity will alter only the right hand region and the matching solution. The geometrical configuration is as shown in Figure 2.7.

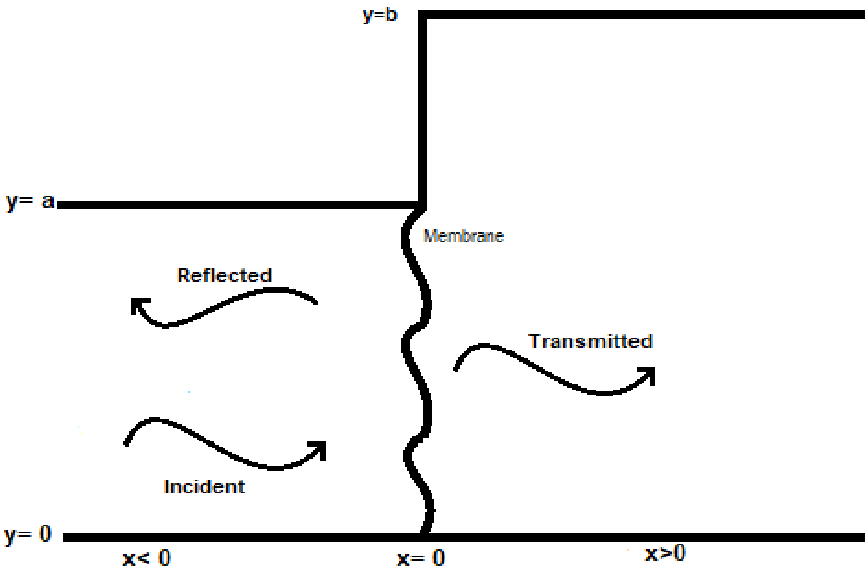

Figure 2.7: The physical configuration of problem-2.

The acoustically rigid step-discontinuity can be defined by

$$\frac{\partial \psi_2}{\partial x} = 0, \quad x = 0, a \leqslant y \leqslant b. \tag{2.60}$$

Therefore, we can write the expansion form for this problem as

$$\psi_2\left(x, y\right) = \sum_{n=0}^{\infty} B_n e^{is_n x} \cos(\gamma_n y), \tag{2.61}$$

for right hand duct, where $s_n = \sqrt{1 - \gamma_n^2}$ is the n^{th} mode wave number in which $\gamma_n = n\pi/b; n = 0, 1, 2, ...$ are the eigenvalues. The corresponding eigenfunctions $\cos(\gamma_n y); n = 0, 1, 2, ...$ satisfy the orthogonality relation

$$\int_0^b \cos(\gamma_n y) \cos(\gamma_m y) dy = \frac{b}{2} \delta_{nm} \varepsilon_m, \tag{2.62}$$

where δ_{mn} is Kronecker delta and $\varepsilon_m = 2$, for $m = 1$ and $\varepsilon_m = 1$, for $m \neq 0$. The amplitudes of the problem can be found using mode-matching technique of pressure and velocity.

2.2.1 Mode-matching

From the continuity of normal velocities at interface, we write

$$\frac{\partial \psi_2}{\partial x}(0,y) = \begin{cases} \frac{\partial \psi_1}{\partial x}, & 0 \leqslant y \leqslant a, \\ 0, & a \leqslant y \leqslant b. \end{cases} \tag{2.63}$$

On using (2.27) and (2.61) into (2.63), we obtain

$$\sum_{n=0}^{\infty} iB_n s_n \cos(\gamma_n y) = \begin{cases} \sum_{n=0}^{\infty} \{F_n - A_n\} i\eta_n \cos(\tau_n y), & 0 \leqslant y \leqslant a, \\ 0, & a \leqslant y \leqslant b. \end{cases} \tag{2.64}$$

On multiplying (2.64) with $\cos(\gamma_m y)$, integrating over $0 \leqslant y \leqslant b$ and then using orthogonality relation (2.62), we get

$$B_m = \frac{2}{s_m \varepsilon_m b} \sum_{n=0}^{\infty} F_n \eta_n R_{mn} - \frac{2}{s_m \varepsilon_m b} \sum_{n=0}^{\infty} A_n \eta_n R_{mn}, \tag{2.65}$$

where

$$R_{mn} = \int_0^b \cos(\gamma_m y) \cos(\tau_n y) dy. \tag{2.66}$$

Now, for $A_n; n = 0, 1, 2 \ldots$, we invoke (2.27) and (2.61) into (2.35) to get

$$-\sum_{n=0}^{\infty} \kappa_n B_n \cos(\gamma_n y) + \alpha \sum_{n=0}^{\infty} F_n \cos(\tau_n y) + \alpha \sum_{n=0}^{\infty} A_n \cos(\tau_n y) = 2\delta(y) E_1 + 2\delta(y-a) E_2, \tag{2.67}$$

where

$$\kappa_n = is_n \left(\gamma_n^2 - \mu^2\right) + \alpha.$$

On multiplying (2.67) with $\cos(\tau_m y)$, integrating over $0 \leqslant y \leqslant a$ and then using orthogonality relation (2.32), we found

$$A_m = -F_m + \frac{2}{\varepsilon_m a \alpha} \sum_{n=0}^{\infty} \kappa_n B_n R_{nm} + \frac{2}{\varepsilon_m a \alpha} E_1 + \frac{2}{\varepsilon_m a \alpha} E_2 (-1)^m. \tag{2.68}$$

Note that the constants E_1 and E_2 are still unknown. These are determined through the physical connection of vertical membrane with horizontal rigid plate. Let us assume here the edges to be fixed, thus displacement is zero, that is,

$$\frac{\partial \psi_1}{\partial x} = 0, \quad x = 0, \quad y = 0, \tag{2.69}$$

and

$$\frac{\partial \psi_1}{\partial x} = 0, \quad x = 0, \quad y = a. \tag{2.70}$$

On differentiating (2.27) with respect to x, we get

$$\phi_{1x}(x, y) = \sum_{n=0}^{\infty} iF_n e^{-i\eta_n x}\eta_n - \sum_{n=0}^{\infty} iA_n e^{-i\eta_n x}\eta_n \cos(\tau_n y)\,. \tag{2.71}$$

On using (2.71) into (2.69) and (2.70), we obtain

$$\sum_{m=0}^{\infty} A_m \eta_m = \sum_{m=0}^{\infty} F_m \eta_m, \tag{2.72}$$

and

$$\sum_{m=0}^{\infty} A_m \eta_m (-1)^m = \sum_{m=0}^{\infty} F_m (-1)^m \eta_m. \tag{2.73}$$

Now, we multiply (2.68) with $\sum_{m=0}^{\infty} \eta_m$ and then substitute (2.72) which after little simplification yields

$$S_1 E_1 + S_2 E_2 = 2\sum_{m=0}^{\infty} F_m \eta_m - \sum_{n=0}^{\infty}\sum_{m=0}^{\infty} \frac{2}{\varepsilon_m a\alpha}\eta_m \kappa_n B_n R_{nm}, \tag{2.74}$$

where

$$S_1 = \sum_{m=0}^{\infty} \frac{2\eta_m}{a\varepsilon_m \alpha},$$

and

$$S_2 = \sum_{m=0}^{\infty} \frac{2\eta_m}{a\varepsilon_m \alpha}(-1)^m.$$

To enforce (2.73), again we multiply (2.68) with $\sum_{m=0}^{\infty} i\eta_m(-1)^m$ and then use (2.73) to get

$$S_2E_1 + S_1E_2 = 2\sum_{n=0}^{\infty} F_m\eta_m(-1)^m - \sum_{n=0}^{\infty}\sum_{m=0}^{\infty} \frac{2}{\varepsilon_m a\alpha}\eta_m(-1)^m B_n R_{nm}\kappa_n. \quad (2.75)$$

In this way E_1 and E_2 are found after solving (2.74) and (2.75) simultaneously. Let us assume the incident forcing $F_m = \delta_{mo}$ which cater only the fundamental duct mode to be incident, the expressions (2.65) and (2.68) yield the reflected and transmitted amplitudes, respectively.

2.2.2 Energy Conservation

The power components for incident and reflected fields remain same as defined in (2.46) and (2.50). However, the expression for transmitted power is different. This can be calculated by using (2.61) in (2.45), and then simplifying the resulting with aid of orthogonality relation (2.62) reveals

$$P_t = \frac{b}{4}Re\left[\sum_{n=0}^{\infty} \mid B_n \mid^2 \varepsilon_n s_n\right]. \quad (2.76)$$

From the fact that left hand side power must be equal to right hand side power leads to

$$\frac{a}{2} = \frac{b}{4}Re\left[\sum_{n=0}^{\infty} \mid B_n \mid^2 \varepsilon_n s_n\right] + \frac{a}{4}Re\left[\sum_{n=0}^{\infty} \mid A_n \mid^2 \varepsilon_n \eta_n\right]. \quad (2.77)$$

In order to scale the incident power at unity we multiply (2.77) with $2/a$ to get

$$1 = \mathcal{E}_r + \mathcal{E}_t, \quad (2.78)$$

where,

$$\mathcal{E}_r = \frac{1}{2}Re\left[\sum_{n=0}^{\infty} \mid A_n \mid^2 \varepsilon_n \eta_n\right]$$

and

$$\mathcal{E}_t = \frac{b}{2a}Re\left[\sum_{n=0}^{\infty} \mid B_n \mid^2 \varepsilon_n s_n\right].$$

Note that (2.78) is known as the conserved power identity.

2.2.3 Numerical Results

To discuss the problem numerically, we truncate the infinite system of equations defined by (2.65) and (2.68) along with (2.74) and (2.75) upto $n = m = 0; 1, 2, \ldots, N$ terms. So it clearly reveals $N + 1$ equations. To draw the results graphically, considered system is truncated upto $N = 50$ terms. The physical parameters to plot these graphs remain same as given in previous problem. The dimensional duct heights $\bar{a} = 0.08$ and $\bar{b} = 0.1$ remain fixed. The real and imaginary parts of normal velocities versus non-dimensional duct heights at interface for fixed frequency $f = 250$Hz are illustrated in Figures 2.8 and 2.9, respectively.

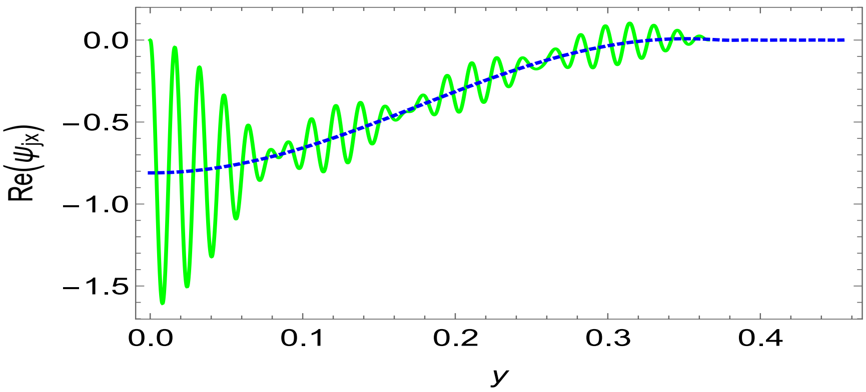

Figure 2.8: Real part of normal velocity plotted against duct height y, where $\bar{a} = 0.08$ and $\bar{b} = 0.1$.

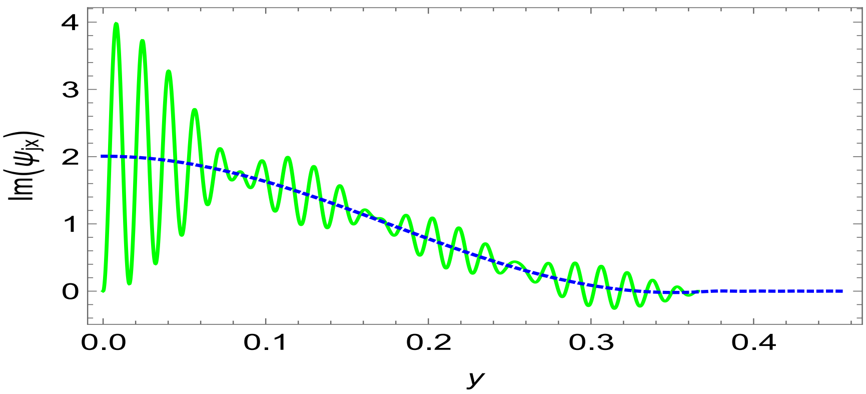

Figure 2.9: Imaginary part of normal velocity plotted against duct height y, where $\bar{a} = 0.08$ and $\bar{b} = 0.1$.

It can be seen that, both the curves coincide which clearly reveals that the truncated solution reconstructs exactly the matching condition (2.63). Moreover, it confirms the accuracy of the performed algebra. To understand the problem physically, the reflected and transmitted powers are plotted against frequency for different values of tension. It can be seen that, by varying frequency from 1Hz to 1000Hz, a significant variation in power components is noted. Also by changing the tension T of the membrane, the dips points are varied. Moreover the sum of reflected and transmitted power is unity as assumed in (2.57). It clearly justifies the conservation of power computationally. The results of power against frequencies for different values of tensions T = 350N, T = 3500N and T = 7500N are shown in the Figures 2.10, 2.11 and 2.12, respectively.

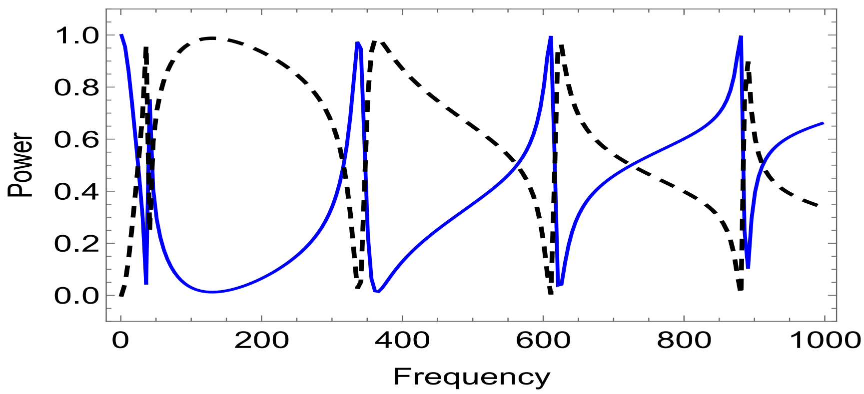

Figure 2.10: Reflected power $\mathcal{E}_r$ (solid line) and transmitted power $\mathcal{E}_t$ (dashed line) against frequency for tension T = 350N, where, $\bar{a} = 0.08$ and $\bar{b} = 0.1$.

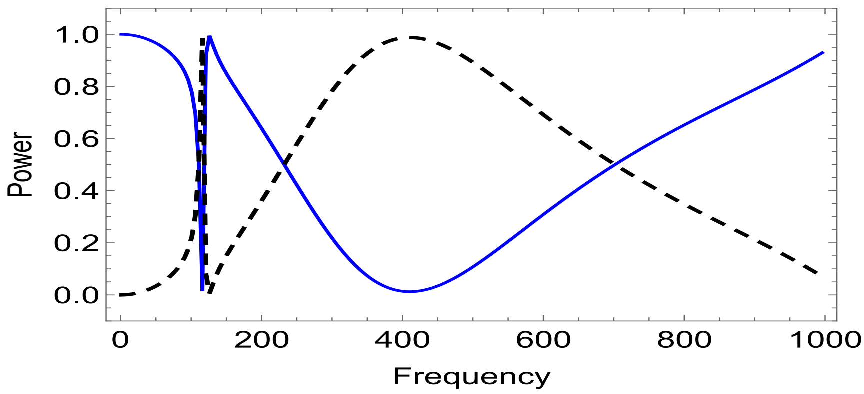

Figure 2.11: Reflected power $\mathcal{E}_r$ (solid line) and transmitted power $\mathcal{E}_t$ (dashed line) against frequency for tension T = 3500N, where, $\bar{a} = 0.08$ and $\bar{b} = 0.1$.

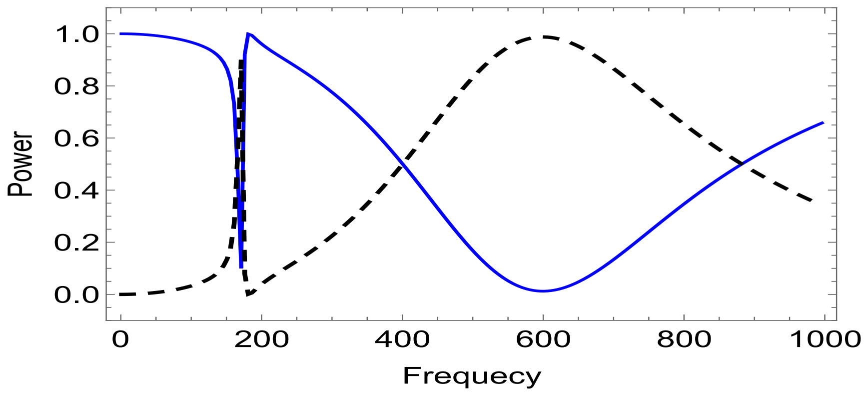

Figure 2.12: Reflected power $\mathcal{E}_r$ (solid line) and transmitted power $\mathcal{E}_t$ (dashed line) against frequency for tension $\mathrm{T} = 7500\mathtt{N}$, where, $\bar{a} = 0.08$ and $\bar{b} = 0.1$.

It can be seen that by varying tension of vertical membrane, a significant variation in scattering powers is observed.

Chapter 3

Reflection and Transmission Through Expansion Chamber Enclosed by Vertical Membranes

In this chapter, we consider the propagation and scattering of acoustic waves through an expansion chamber containing vertical membrane barriers at the junctions of infinite waveguide. The waveguide is bounded above and below by rigid walls and contains three sections. For convenience, the main problem is divided into two sub-problems that are symmetric and anti-symmetric cases. The mathematical modeling of each sub-problem and its solution is discussed in subsequent sections. At the end the results of both sub-problems are combined to obtain the result of the problem.

3.1 Mathematical Formulation

In this problem, we consider a rigid waveguide with expansion chamber having vertical membranes at junctions. The length of the expansion chamber is $2L$ and its junctions are at $\pm L$. The problem contains three sections inlet section, expansion chamber and outlet section. The geometrical configuration is as shown in Figure 3.1.

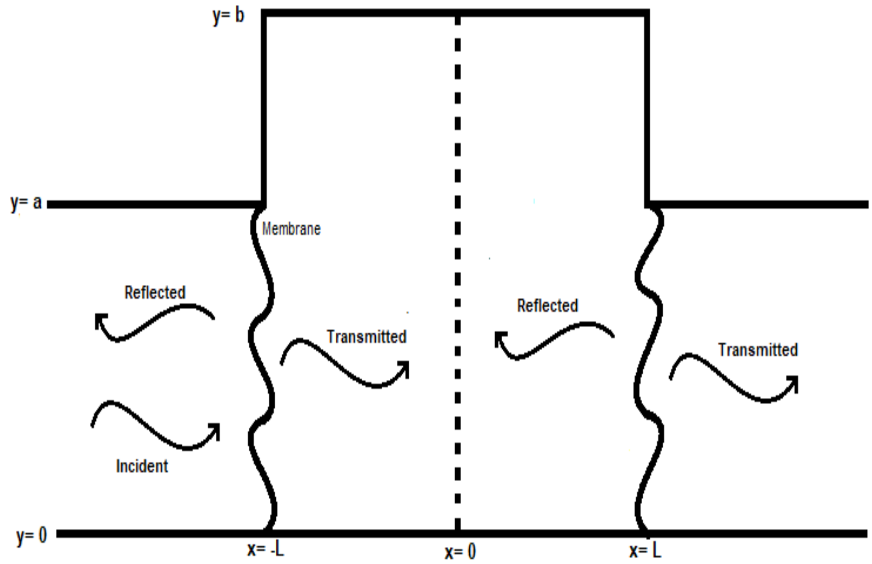

Figure 3.1: The physical configuration of problem.

Consider an incident wave is propagating from the inlet towards the expansion chamber which after interaction with expansion chamber will transmit in the outlet section. The governing equation is Helmholtz equation along with rigid boundary conditions. These are non-dimensionalized in similar way as discussed in Chapter 2. Also, the harmonic time dependence is assumed. The non-dimensional form of boundary value problem is

$$\left\{\nabla^2 + 1\right\}\psi_j = 0, \quad j = 1,2,3, \quad -\infty < x < \infty, \tag{3.1}$$

$$\frac{\partial \psi_1}{\partial y} = 0, \quad y = 0, a, \quad x < -L, \tag{3.2}$$

$$\frac{\partial \psi_2}{\partial y} = 0, \quad y = 0, b, \quad \mid x \mid < L, \tag{3.3}$$

$$\frac{\partial \psi_3}{\partial y} = 0, \quad y = 0, a', \quad x > L. \tag{3.4}$$

At junctions $x = \pm L, 0 \leqslant y \leqslant a$, the non-dimensional form of membrane boundaries are given by

$$\left\{\frac{\partial^2}{\partial y^2} + \mu^2\right\} \frac{\partial \psi_2}{\partial x} - \alpha \left[\psi_2 - \psi_1\right] = 2E_1 \delta\left(y\right) + 2E_2 \delta\left(y - a\right), \tag{3.5}$$

where

$$\frac{\partial \psi_1}{\partial x} = \frac{\partial \psi_2}{\partial x}, \quad x = -L,$$

and

$$\frac{\partial \psi_2}{\partial x} = \frac{\partial \psi_3}{\partial x}, \quad x = L.$$

Moreover, the edges of vertical membranes are fixed, that are

$$\frac{\partial \psi_2}{\partial x} = 0, \quad x = \pm L, \quad y = 0, a. \tag{3.6}$$

Note that $\psi_1(x, y)$, $\psi_2(x, y)$ and $\psi_3(x, y)$ denote velocity potentials in inlet, expansion chamber and outlet, respectively. The eigenfunction expansion form of these fluid potentials are

$$\psi_1\left(x, y\right) = \sum_{n=0}^{\infty} \left\{F_n e^{i\eta_n(x+L)} + A_n e^{-i\eta_n(x+L)}\right\} \cos(\tau_n y), \tag{3.7}$$

$$\psi_2\left(x, y\right) = \sum_{n=0}^{\infty} \left\{B_n e^{is_n x} + C_n e^{-is_n x}\right\} \cos(\gamma_n y), \tag{3.8}$$

and

$$\psi_3\left(x, y\right) = \sum_{n=0}^{\infty} D_n e^{i\eta_n(x-L)} \cos(\tau_n y), \tag{3.9}$$

where $\eta_n = \sqrt{1 - \tau_n^2}$ and $s_n = \sqrt{1 - \gamma_n^2}$ are the wave numbers. Note that the first term in (3.7) represents the incident wave with forcing F_n (that will be defined later) whereas the second term shows the reflected field in the inlet. Here, $\{A_n, B_n, C_n, D_n\}$ are unknowns. These are found through the mode-matching of pressure and velocity modes at interfaces. However, before doing this, we divide the problem into two sub-problems, i.e., symmetric case and anti-symmetric case. The division is done by considering a forcing wave located at inlet duct impinging on membrane. This wave travels from positive to negative x-direction which is negative in anti-symmetric sub-problem because of a phase shift π (Euler 's identity). The reduced sub-problems are easy to solve as compared to the original problem.

3.2 Symmetric Case

In this section, we consider a symmetric semi-infinite sub-problem with an abrupt change in height having vertical membrane present at junction $x = -L, 0 \leqslant y \leqslant a$. The sub-problem is enclosed by rigid wall located at $x = 0$ and contains two sections as shown in Figure 3.2.

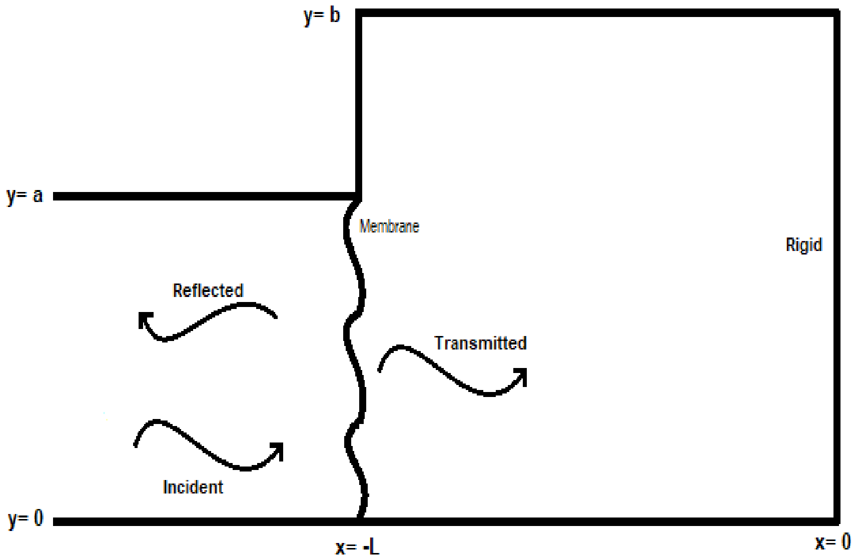

Figure 3.2: The physical configuration of a symmetric sub-problem.

The expansion forms of eigenfunctions for this symmetric sub-problem are

$$\psi_1^s(x, y) = \sum_{n=0}^{\infty} \left\{ F_n^s e^{i\eta_n(x+L)} + A_n^s e^{-i\eta_n(x+L)} \right\} \cos(\tau_n y), \tag{3.10}$$

and

$$\psi_2^s(x, y) = \sum_{n=0}^{\infty} \left\{ B_n^s e^{is_n x} + C_n^s e^{-is_n x} \right\} \cos(\gamma_n y). \tag{3.11}$$

Here, $\{A_n^s, B_n^s, C_n^s\}$ are unknown amplitudes for symmetric case. The boundary condition for rigid wall located at $x = 0$ is given by

$$\frac{\partial \psi_2^s}{\partial x}(0, y) = 0. \tag{3.12}$$

On using (3.11) into (3.12), we get

$$B_n^s = C_n^s. \tag{3.13}$$

On using (3.13), (3.11) leads to

$$\psi_2^s(x, y) = \sum_{n=0}^{\infty} 2B_n^s \cos(s_n x)\cos(\gamma_n y). \tag{3.14}$$

Now our unknowns become $\{A_n^s, B_n^s\}$. These will be found through matching conditions in the next section.

3.2.1 Mode-matching

Here we match the pressures and normal velocities modes at interface $x = -L$. From the continuity of normal velocities at $x = -L$, we may write

$$\frac{\partial \psi_2^s}{\partial x}(-L, y) = \begin{cases} \frac{\partial \psi_1^s}{\partial x}(-L, y), & 0 \leqslant y \leqslant a, \\ 0, & a \leqslant y \leqslant b. \end{cases} \tag{3.15}$$

By using (3.10) and (3.14) into (3.15), we get

$$\sum_{n=0}^{\infty} 2B_n^s \sin(s_n L) s_n \cos(\gamma_n y) = \begin{cases} \sum_{n=0}^{\infty}\{F_n^s - A_n^s\} i\eta_n \cos(\tau_n y), & 0 \leqslant y \leqslant a, \\ 0, & a \leqslant y \leqslant b. \end{cases} \tag{3.16}$$

On multiplying (3.16) with $\cos(\gamma_m y)$ and integrating over $0 \leqslant y \leqslant b$ and then using (2.62), we get

$$B_m^s = \frac{i}{b s_m \sin(s_m L) \varepsilon_m} \sum_{n=0}^{\infty} \{F_n^s - A_n^s\} \eta_n R_{mn}. \tag{3.17}$$

We discuss the pressure across the region for membrane junction at $x = -L, 0 \leqslant y \leqslant a$. We substitute (3.10) and (3.14) into membrane boundary condition (3.5)

$$-\sum_{n=0}^{\infty} 2\xi_n B_n^s \cos(\gamma_n y) + \alpha \sum_{n=0}^{\infty} F_n^s \cos(\tau_n y) + \alpha \sum_{n=0}^{\infty} A_n^s \cos(\tau_n y)$$
$$= 2\delta(y) E_1 + 2\delta(y-a) E_2, \tag{3.18}$$

where,

$$\xi_n = \sin(s_n L) s_n \left(\gamma_n^2 - \mu^2\right) + \alpha \cos(s_n L).$$

On multiplying (3.18) with $\cos(\tau_m y)$ and integrating over $0 \leqslant y \leqslant a$ and then using orthogonality relation (2.32), we get

$$A_m^s = -F_m^s + \frac{4}{\varepsilon_m \alpha a} \sum_{n=0}^{\infty} \xi_n B_n^s R_{nm} + \frac{2E_1}{\varepsilon_m \alpha a} + \frac{2E_2(-1)^m}{\varepsilon_m \alpha a}. \tag{3.19}$$

Note that the constants E_1 and E_2 are still unknowns. These are determined through the physical connection of vertical membrane with horizontal rigid plate. Here, we assume the edges to be fixed, thus

$$\frac{\partial \psi_1^s}{\partial x}(-L, 0) = 0, \tag{3.20}$$

and

$$\psi_{1x}^s(-L, a) = 0. \tag{3.21}$$

On differentiating (3.10) with respect to x, we found

$$\frac{\partial \psi_1^s}{\partial x}(x, y) = i \sum_{m=0}^{\infty} \left\{F_m^s e^{i\eta_m(x+L)} - A_m^s e^{-i\eta_m(x+L)}\right\} \eta_m \cos(\tau_m y). \tag{3.22}$$

On using (3.22) into (3.20) and (3.21), we obtain

$$\sum_{m=0}^{\infty} A_m^s \eta_m = \sum_{m=0}^{\infty} F_m^s \eta_m, \tag{3.23}$$

and

$$\sum_{m=0}^{\infty} A_m^s \eta_m (-1)^m = \sum_{m=0}^{\infty} F_m^s \eta_m (-1)^m. \tag{3.24}$$

To enforce (3.23), we multiply (3.19) with $\sum_{m=0}^{\infty} \eta_m$ and then simplify the result with the aid of (3.23), which yields

$$S_1 E_1 + S_2 E_2 = 2\sum_{m=0}^{\infty} F_m^s \eta_m - \sum_{m=0}^{\infty}\sum_{n=0}^{\infty} \frac{4\eta_m}{\varepsilon_m \alpha a} B_n^s R_{nm} \xi_n, \tag{3.25}$$

where

$$S_1 = \sum_{m=0}^{\infty} \frac{2\eta_m}{\varepsilon_m \alpha a},$$

and

$$S_2 = \sum_{m=0}^{\infty} \frac{2\eta_m (-1)^m}{\varepsilon_m \alpha a}.$$

Similarly, to enforce (3.24), we multiply (3.19) with $\sum_{m=0}^{\infty} \eta_m (-1)^m$ and then simplifying the result using (3.24) to get

$$S_2 E_1 + S_1 E_2 = 2\sum_{m=0}^{\infty} F_m^s \eta_m (-1)^m - \sum_{m=0}^{\infty}\sum_{n=0}^{\infty} \frac{4\eta_m (-1)^m}{\varepsilon_m \alpha a} B_n^s R_{nm} \xi_n. \tag{3.26}$$

Here, E_1 and E_2 are found after solving (3.25) and (3.26) simultaneously. If we assume incident forcing, $F_m = \delta_{m0}$, which cater only fundamental duct mode to be incident, the expressions (3.17) and (3.19) yield the reflected and transmitted amplitudes, respectively.

3.3 Anti-symmetric Case

In anti-symmetric case, the rigid wall present at $x = 0$ in symmetric sub-problem is replaced by acoustically soft wall as shown in Figure 3.3.

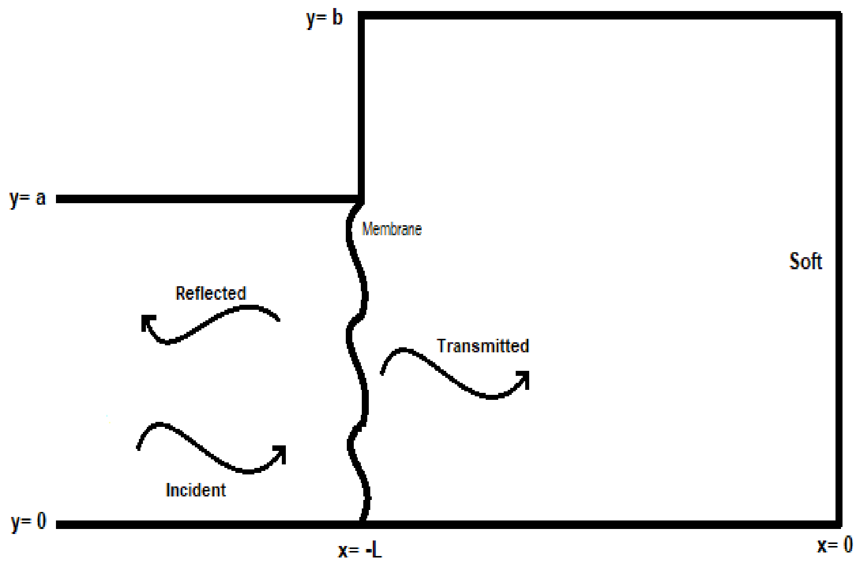

Figure 3.3: The physical configuration of an anti-symmetric sub-problem.

The eigenfunctions expansion forms for anti-symmetric sub-problem are

$$\psi_1^a(x,y) = \sum_{n=0}^{\infty} \left\{ F_n^a e^{i\eta_n(x+L)} + A_n^a e^{-i\eta_n(x+L)} \right\} \cos(\tau_n y), \tag{3.27}$$

and

$$\psi_2^a(x,y) = \sum_{n=0}^{\infty} \left\{ B_n^a e^{is_n x} + C_n^a e^{-is_n x} \right\} \cos(\gamma_n y). \tag{3.28}$$

Here, (A_n^a, B_n^a, C_n^a) are unknown amplitudes for anti-symmetric case. The boundary condition for soft wall located at $x = 0$ is given by

$$\psi_2^a(0,y) = 0. \tag{3.29}$$

On using (3.28) into (3.29), we get

$$C_n^a = -B_n^a. \tag{3.30}$$

On using (3.30), (3.28) leads to

$$\psi_2^a(x,y) = \sum_{n=0}^{\infty} 2iB_n^a \sin(s_n x) \cos(\gamma_n y). \tag{3.31}$$

Here, our unknowns become $\{A_n^a, B_n^a\}$. These will be found through matching conditions in the next section.

3.3.1 Mode-matching

Here we match the pressure and normal velocity modes at interface to determine $\{A_n^a, B_n^a\}$. From the continuity of normal velocities at $x = -L$, we may write

$$\frac{\partial \psi_2^a}{\partial x}(-L, y) = \begin{cases} \frac{\partial \psi_1^a}{\partial x}(-L, y), & 0 \leqslant y \leqslant a, \\ 0, & a \leqslant y \leqslant b. \end{cases} \tag{3.32}$$

By using (3.27) and (3.31) into (3.32), we get

$$\sum_{n=0}^{\infty} 2iB_n^a \cos(s_n L) s_n \cos\left(\gamma_n^2 y\right) = \begin{cases} \sum_{n=0}^{\infty} \{F_n^a - A_n^a\} i\eta_m \cos(\tau_n y), 0 \leqslant y \leqslant a \\ 0, & a \leqslant y \leqslant b. \end{cases} \tag{3.33}$$

On multiplying (3.33) with $\cos(\gamma_m y)$ and integrating over $0 \leqslant y \leqslant b$ and then by using the orthogonality relation (2.62), which results

$$B_m^a = \frac{1}{bs_m \cos(s_m L) \varepsilon_m} \sum_{n=0}^{\infty} \{F_n^a - A_n^a\} \eta_n R_{mn}. \tag{3.34}$$

Now, we discuss the pressure across the region for membrane junction at $x = -L, 0 \leqslant y \leqslant a$. We substitute (3.27) and (3.31) into membrane boundary condition (3.5) to obtain

$$-\sum_{n=0}^{\infty} 2i\Omega_n B_n^a \cos(\gamma_n y) + \alpha \sum_{n=0}^{\infty} F_n^a \cos(\tau_n y) + \alpha \sum_{n=0}^{\infty} A_n^a \cos(\tau_n y) = 2\delta(y)E_1 + 2\delta(y-a)E_2, \tag{3.35}$$

where

$$\Omega_n = \left(\gamma_n^2 - \mu^2\right) \cos(s_n L) s_n - \alpha \sin(s_n L).$$

On multiplying (3.35) with $\cos(\tau_m y)$ and integrating over $0 \leqslant y \leqslant a$ and using orthogonality relation (2.32), we get

$$A_m^a = -F_m^a + \frac{2E_1}{\varepsilon_m \alpha a} + \frac{2E_2(-1)^m}{\varepsilon_m \alpha a} + \frac{4i}{\varepsilon_m \alpha a} \sum_{n=0}^{\infty} B_n^a R_{nm} \Omega_n. \tag{3.36}$$

Note that the constants E_1 and E_2 are still unknown. These are determined through physical connection of vertical membrane with horizontal rigid plate. Here, we assume the edges to be fixed, that is,

$$\frac{\partial \psi_1^a}{\partial x}(x, y) = 0, \quad x = -L, \quad y = 0, \tag{3.37}$$

and

$$\frac{\partial \psi_1^a}{\partial x}(x, y) = 0, \quad x = -L, \quad y = a. \tag{3.38}$$

On differentiating (3.27) with respect to x, we get

$$\psi_{1x}^a(x, y) = i \sum_{m=0}^{\infty} \left\{ F_m^a e^{i\eta_m(x+L)}) - A_m^a e^{-i\eta_m(x+L)} \right\} \eta_m \cos(\tau_m y) = 0, \tag{3.39}$$

On using (3.39) into (3.37) and (3.38), we obtain

$$\sum_{m=0}^{\infty} A_m^a \eta_m = \sum_{m=0}^{\infty} F_m^a \eta_m, \tag{3.40}$$

and

$$\sum_{m=0}^{\infty} A_m^a \eta_m (-1)^m = \sum_{m=0}^{\infty} F_m^a \eta_m (-1)^m. \tag{3.41}$$

To enforce (3.40), we multiply (3.36) with $\sum_{m=0}^{\infty} \eta_m$ and then by simplifying the result with the aid of (3.40) yields

$$S_1 E_1 + S_2 E_2 = 2 \sum_{m=0}^{\infty} F_m^a \eta_m - \frac{4i}{a\alpha} \sum_{m=0}^{\infty} \sum_{n=0}^{\infty} \frac{\eta_m}{\varepsilon_m} B_n^a R_{nm} \Omega_n, \tag{3.42}$$

where

$$S_1 = \sum_{m=0}^{\infty} \frac{2\eta_m}{\varepsilon_m \alpha a},$$

and

$$S_2 = \sum_{m=0}^{\infty} \frac{2\eta_m(-1)^m}{\varepsilon_m \alpha a}.$$

Similarly, to enforce (3.41), we multiply (3.36) with $\sum_{m=0}^{\infty} \eta_m(-1)^m$ and then simplifying the result using (3.41) we get

$$S_2E_1 + S_1E_2 = 2\sum_{m=0}^{\infty} F_m^a \eta_m(-1)^m - \frac{4i}{a\alpha}\sum_{m=0}^{\infty}\sum_{n=0}^{\infty} \frac{\eta_m(-1)^m}{\varepsilon_m} B_n^a R_{nm}\Omega_n. \tag{3.43}$$

E_1 and E_2 are found after solving (3.42) and (3.43) simultaneously. If we assume incident forcing $F_m = \delta_{m0}$, which cater only the fundamental duct mode to be incident, the expressions (3.34) and (3.36) yield the reflected and transmitted amplitudes, respectively.

The amplitudes of reflected and transmitted waves in inlet and outlet ducts respectively of the problem can be found by adding and subtracting the amplitudes of reflected waves in symmetric and anti-symmetric sub-problems. So the reflected and transmitted amplitudes of main problem are

$$A_m = \frac{A_m^s + A_m^a}{2}, \tag{3.44}$$

and

$$D_m = \frac{A_m^s - A_m^a}{2}, \tag{3.45}$$

respectively.

3.4 Energy Conservation

The power components for incident and reflected fields remain same as defined in (2.47) and (2.48). However, the expression for transmitted power is different. The eigenfunction expansion form for transmitted field is

$$\psi_t(x, y) = \sum_{n=0}^{\infty} D_n \cos(\tau_n y)\, e^{i\eta_n(x-L)}. \tag{3.46}$$

The transmitted power can be calculated by using (3.46) into (2.45) and then by simplifying the result with the aid of orthogonality relation (2.62), which reveals

$$P_t = \frac{a}{4} Re \left[\sum_{n=0}^{\infty} \mid D_n \mid^2 \varepsilon_n \eta_n \right]. \tag{3.47}$$

Now, the fact that the left hand side power must be equal to the right hand side power leads to

$$\frac{a}{2} = \frac{a}{4} Re \left[\sum_{n=0}^{\infty} \mid D_n \mid^2 \varepsilon_n \eta_n \right] + \frac{a}{4} Re \left[\sum_{n=0}^{\infty} \mid A_n \mid^2 \varepsilon_n \eta_n \right]. \tag{3.48}$$

In order to scale the incident power at unity, we multiply (3.48) with $2/a$ to get

$$1 = \mathcal{E}_t + \mathcal{E}_r, \tag{3.49}$$

which is the power identity, where

$$\mathcal{E}_r = \frac{1}{2} Re \left[\sum_{n=0}^{\infty} \mid A_n \mid^2 \varepsilon_n \eta_n \right],$$

and

$$\mathcal{E}_t = \frac{1}{2} Re \left[\sum_{n=0}^{\infty} \mid D_n \mid^2 \varepsilon_n \eta_n \right].$$

3.5 Numerical Results

In this section, we truncate the infinite system of equations upto $n = m = 0, 1, 2, \ldots, N$ terms. Therefore, it clearly reveals $N + 1$ equations. Here, the system is truncated upto $N = 50$ terms. The physical parameters to plot the graph remain same as given in previous Chapter. The dimensional duct heights $\bar{a} = 2.8$ and $\bar{b} = 4$ remain fixed. The real and imaginary parts of normal velocities against non-dimensional duct heights at interfaces are illustrated in the Figures 3.4, 3.5, 3.6 and 3.7, respectively for fixed frequency $f = 250$Hz.

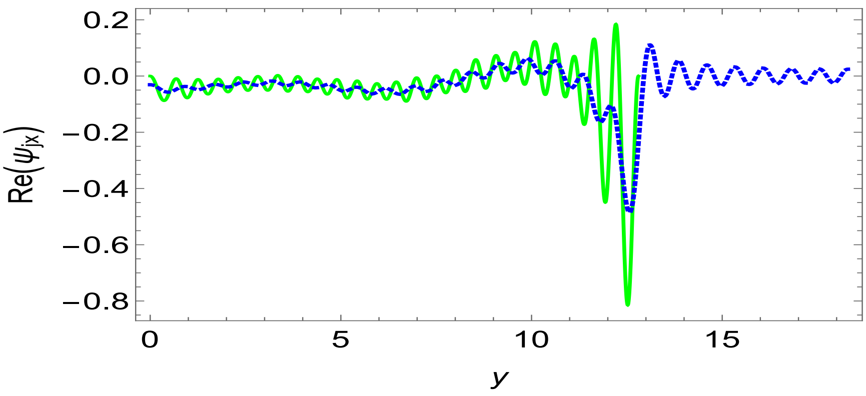

Figure 3.4: Real part of normal velocity plotted against duct height y at $x = -L$, where $\bar{a} = 2.8$ and $\bar{b} = 4$.

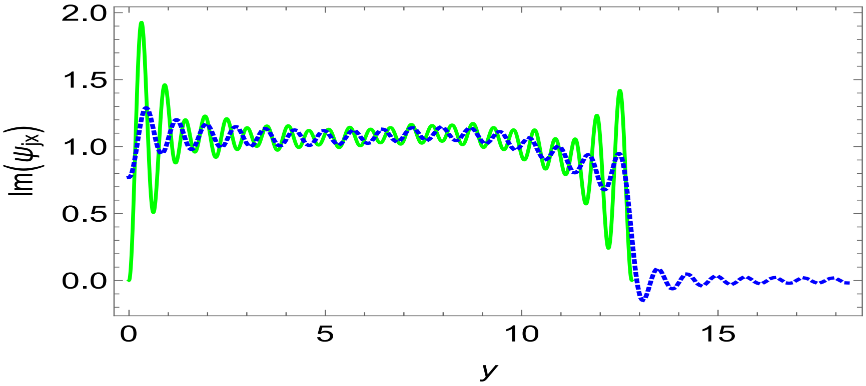

Figure 3.5: Imaginary part of normal velocity plotted against duct height y at $x = -L$, where $\bar{a} = 2.8$ and $\bar{b} = 4$.

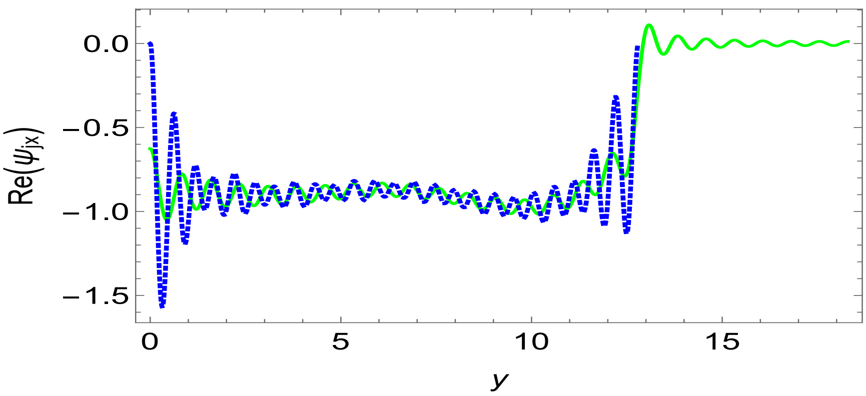

Figure 3.6: Real part of normal velocity plotted against duct height y at $x = L$, where $\bar{a} = 2.8$ and $\bar{b} = 4$.

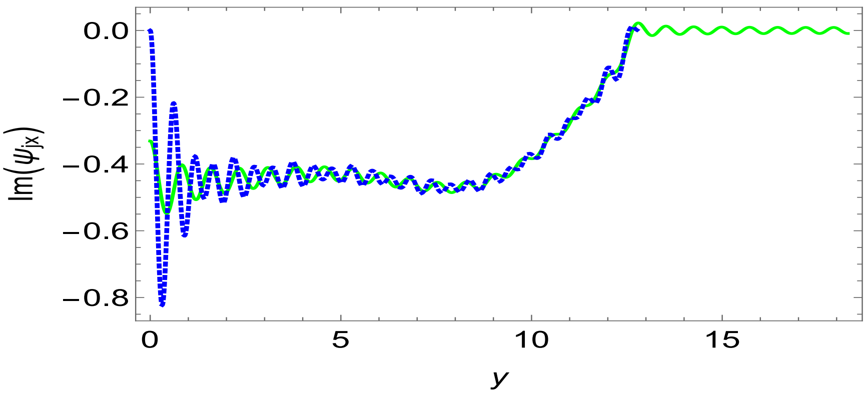

Figure 3.7: Imaginary part of normal velocity plotted against duct height y at $x = L$, where $\bar{a} = 2.8$ and $\bar{b} = 4$.

It can be seen that velocity curves coincide which clearly reveals that the truncated solution reconstructs exactly the matching conditions.

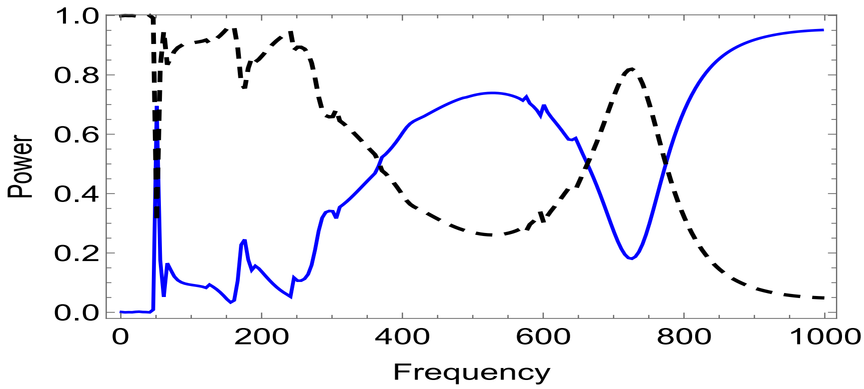

Figure 3.8: Reflected power $\mathcal{E}_r$ (solid line) and transmitted power $\mathcal{E}_t$ (dashed line) against frequency for tension T $= 350\mathtt{N}$, where $\bar{a} = 2.8$, $\bar{b} = 4$ and $\bar{L} = 0.15$.

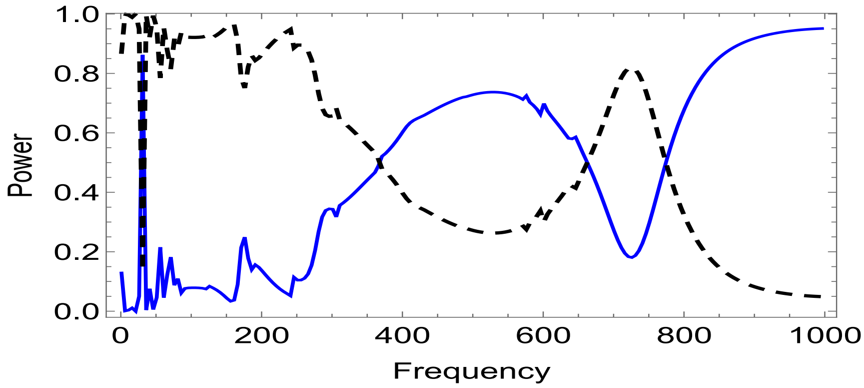

Figure 3.9: Reflected power $\mathcal{E}_r$ (solid line) and transmitted power $\mathcal{E}_t$ (dashed line) against frequency for tension T $= 3500\mathtt{N}$, where $\bar{a} = 2.8$, $\bar{b} = 4$ and $\bar{L} = 0.15$.

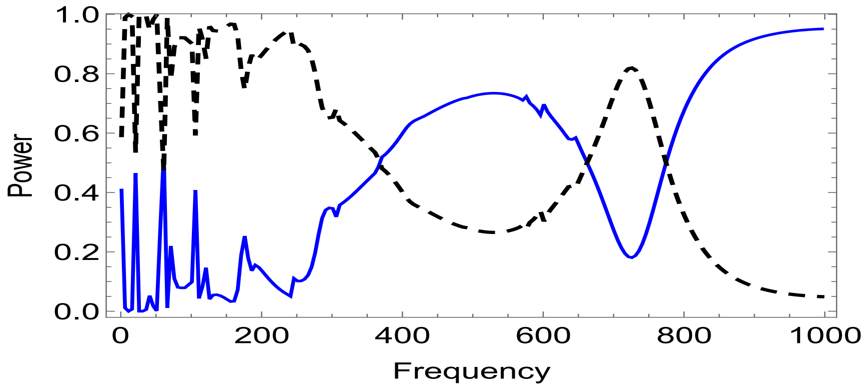

Figure 3.10: Reflected power $\mathcal{E}_r$ (solid line) and transmitted power $\mathcal{E}_t$ (dashed line) against frequency for tension T $= 7500\texttt{N}$, where $\bar{a} = 2.8$, $\bar{b} = 4$ and $\bar{L} = 0.15$.

Moreover, it confirm the accuracy of performed algebra. Now to insight the problem physically, the reflected and transmitted powers are plotted against frequency for different values of tension. It can be seen that by varying frequency from 1Hz to 1000Hz, a significant variation in power components is noted. Also, by changing the tension T of the membrane, the dips points are varied. Moreover, the sum of reflected and transmitted power is unity as assumed in (3.49). It clearly justifies the conservation of power computationally. The results of power against frequencies for different values of tensions T $= 350\texttt{N}$, T $= 3500\texttt{N}$ and T $= 7500\texttt{N}$ are shown in the Figures 3.8, 3.9 and 3.10, respectively.

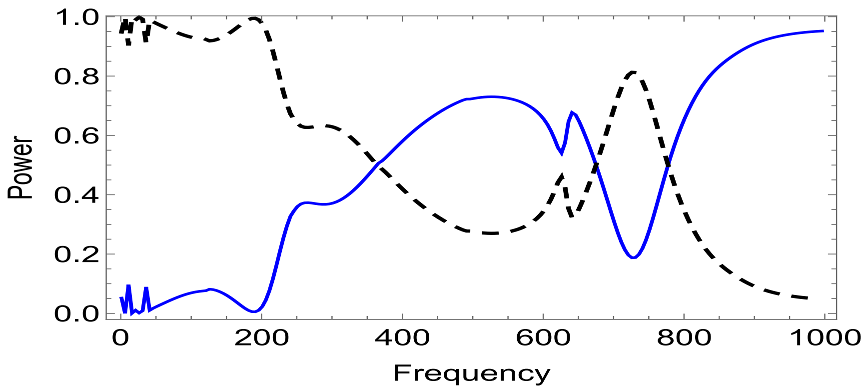

Figure 3.11: Reflected power $\mathcal{E}_r$ (solid line) and transmitted power $\mathcal{E}_t$ (dashed line) against frequency for tension T $= 350\texttt{N}$, where, $\bar{a} = \bar{b} = 2.8$ and $\bar{L} = 0.15$.

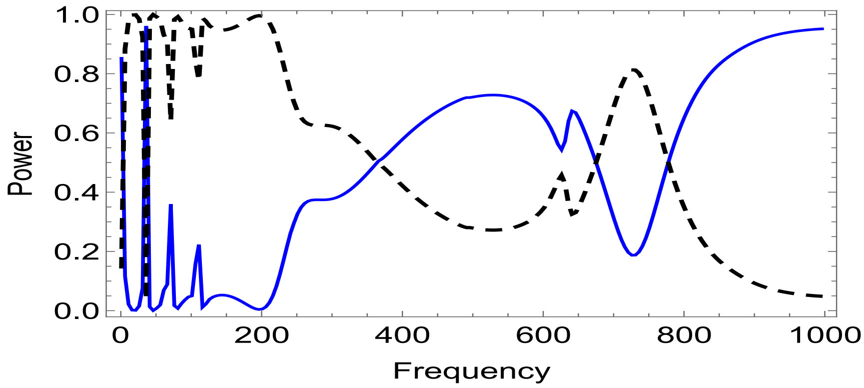

Figure 3.12: Reflected power $\mathcal{E}_r$ (solid line) and transmitted power $\mathcal{E}_t$ (dashed line) against frequency for tension $\mathrm{T} = 3500\mathtt{N}$, where, $\bar{a} = \bar{b} = 2.8$ and $\bar{L} = 0.15$.

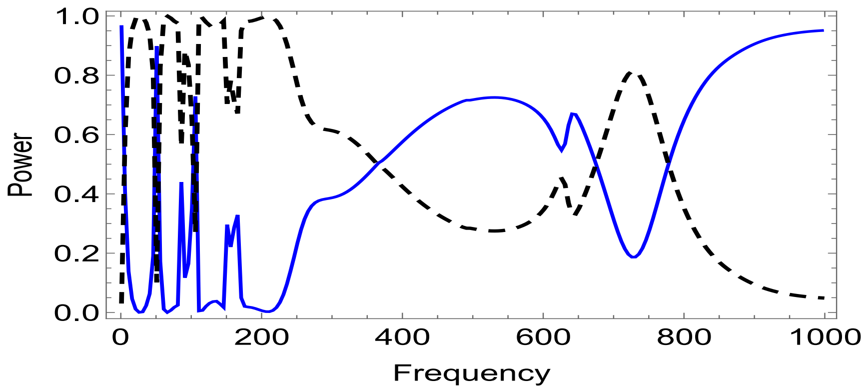

Figure 3.13: Reflected power $\mathcal{E}_r$ (solid line) and transmitted power $\mathcal{E}_t$ (dashed line) against frequency for tension $\mathrm{T} = 7500\mathtt{N}$, where, $\bar{a} = \bar{b} = 2.8$ and $\bar{L} = 0.15$.

When step discontinuity is removed by taking dimensions $\bar{a} = \bar{b} = 2.8$ then the effect of power against frequency for tensions $\mathrm{T} = 350\mathtt{N}$, $\mathrm{T} = 3500\mathtt{N}$ and $\mathrm{T} = 7500\mathtt{N}$ are shown in the Figures 3.11, 3.12 and 3.13 respectively. It can be seen that the behavior of scattering powers in continuous case is different from the discontinuous case. As number of propagating modes vary in both the cases. However, the sum of reflected power in inlet and transmitted power in outlet remains unity.

Chapter 4

Discussion and Conclusion

In this thesis, we have discussed acoustic scattering through an expansion chamber comprising elastic membranes at interfaces. The mode-matching solution has been developed for governing boundary value problem. The involvement of vertical membrane boundaries require imposition of extra conditions on edges of membrane. These condition not only ensure the uniqueness of the solution but also define how the vertical membranes are connected with rigid horizontal surfaces. Thus, to enforce the extra conditions two Dirac delta functions have been considered in the mathematical modeling of the vertical membranes. For fixed edges, the mode-matching solution has been achieved successfully.

In Chapter 2, two problems comprising vertical membrane at $x = 0, 0 \leqslant y \leqslant a$ have been discussed. In first problem continuous waveguide whilst in later case step-discontinuity is additionally involved. Reconstruction of matching conditions for both problems confirm the accuracy of truncated solution. Moreover, the solution is verified later physically through conserved power identity. Additionally, by changing the value of tension, a significant variation in scattering powers is noted.

In Chapter 3, an expansion chamber containing vertical membranes at the ends is considered. Problem is divided into symmetric and anti-symmetric sub-problems. These sub-problems are then solved through mode-matching technique. Scattering of energies are plotted against frequency for continuous and discontinuous expansion chamber. Variation in scattering powers is noted by changing the tension of membranes. Matching conditions are reconstructed and conservation is achieved.

Bibliography

[1] G. Stokes, On the theories of the internal friction of fluids in motion and of the equilibrium and motion of elastic solids, Transactions of the Cambridge Philosophical Society, 8: 75-102 (1845).

[2] H. Helmholtz, On sensations of tone, Longmans Green and company London (1895).

[3] W. Sabine, Reverberation, Reprinted in collected papers on acoustics, Peninsula Publishing Los Altos (1900).

[4] L. Rayleigh and J. Strutt, The theory of sound, Macmillan London (1894), reprinted by Dover (1945).

[5] B. Noble, Methods based on the Wiener-Hopf technique, Pergamon Press London (1958).

[6] R. Beyer, Nonlinear acoustics, American Journal of Physics, 41(9): 1060-1067 (1973).

[7] J. Lighthill, Waves in fluids, Cambridge University Press Cambridge (1978).

[8] N. Rott, Thermoacoustic, Advances in Applied Mechanics, 20: 135-175 (1980).

[9] V. Knudsen and C. Harris, Acoustical designing in architecture, Acoustical Society of America (1980).

[10] A. Cummings and I. Chang, Sound attenuation of a finite length dissipative flow duct silencer with internal mean flow in the absorbent, Journal of Sound and Vibration, 127(1): 1-17 (1988).

[11] Pythagoras, Origins in acoustics, Acoustical Society of America Woodbury (1992).

[12] L. Beranek and D. Martin, Concert and opera halls, how they sound, Journal of the Acoustical Society of America, 99(5): 2637 (1996).

[13] M. Hamilton and D. Blackstock, Nonlinear acoustics, Acoustical Society of America Texas (1998).

[14] J. Lawrie and I. Abrahams, An orthogonality condition for a class of problem with high order boundary conditions, The Quarterly Journal of Mechanics and Applied Mathematics, 52(2): 161-181 (1999).

[15] L. Huang, A theoretical study of duct noise control by flexible panels, Journal of the Acoustical Society of America, 106(6): 1801-1809 (1999).

[16] L. E. Kinsler, A. R. Frey, A. B. Coppens and J. V. Sanders, Fundamentals of acoustics (4th edition), Wiley (2000).

[17] D. Warren, J. Lawrie and I. Mohamed, Acoustic scattering in waveguides with discontinuities in height and material property, Wave Motion, 36(2): 119-142 (2002).

[18] L. Huang, Modal analysis of a drumlike silencer, Journal of the Acoustical Society of America, 112(5): 2014-2025 (2002).

[19] C. Mckinney, The early history of high frequency, short range, high resolution, active sonar, ECHOES 12(2): 4-7 (2002).

[20] L. Huang and Y. Choy, Vibroacoustics of three-dimensional drum silencer, Journal of the Acoustical Society of America, 118(4): 2313-2320 (2005).

[21] T. D. Rossing, Springer handbook of acoustics, Center for Computer Research in Music and Acoustic Stanford (2007).

[22] J. Lawrie, Analytic mode-matching for acoustic scattering in three dimensional waveguides with flexible walls, Wave Motion, 50: 542-557 (2013).

[23] R. Nawaz and J. Lawrie, Scattering of a fluid-structure coupled wave at a flanged junction between two flexible waveguides, Journal of the Acoustical Society of America, 134(3): 1939-1949 (2014).

[24] H. Kim, S.Kim, S. Lee, Y. Seo and P. MaNX , Sound transmission loss of double plates with an air cavity between them in a rigid duct, Journal of the Acoustical Society of America, 139(5): 2324-2333 (2016).

[25] M. Afzal and J. Lawrie, Acoustic scattering in a waveguide with a height discontinuity bridged by a membrane, Journal of Engineering and Applied Mathematics, 105(1): 99-115 (2017).